USDA FOREST SERVICE
GENERAL TECHNICAL REPORT **NC-46**

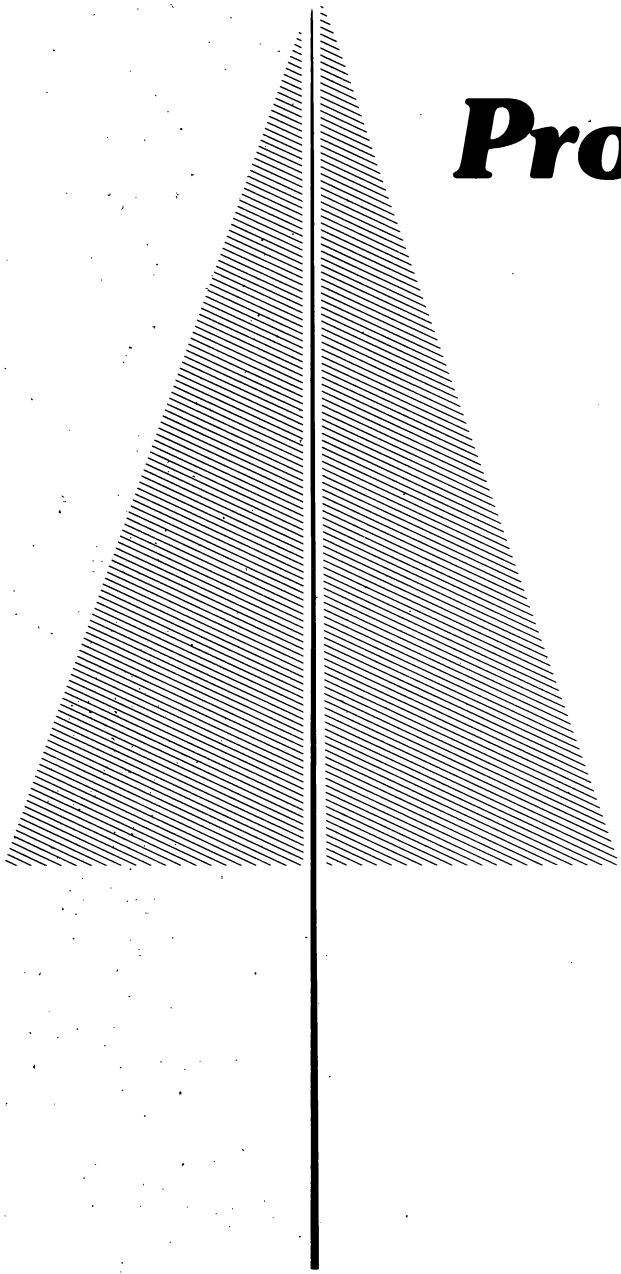

Proceedings

1977 MIDWEST FOREST MENSURATIONISTS Meeting

North Central Forest Experiment Station
Forest Service, U.S. Department of Agriculture

The Midwest Mensurationists are a group of scientists working on quantitative problems in forestry in the mid-section of the country. They meet periodically and informally to discuss matters of mutual interest. The papers included here were presented at their 1977 meeting in Lutsen, Minnesota.

North Central Forest Experiment Station
John H. Ohman, Director
Forest Service - U.S. Department of Agriculture
1992 Folwell Avenue
St. Paul, Minnesota 55108

1978

TABLE OF CONTENTS

Page

Errors in sampling plans based on Wald's Sequential Probability Ratio Test 1
Gary W. Fowler

A comparison of two methods used to estimate stand stocking in upland central hardwoods 14
Robert Rogers

Nonlinear basal area growth models for red pine 17
Chung-Muh Chen and Dietmar W. Rose

Discrete time Markov processes 21
John W. Moser, Jr.

An accurate way to select sample plots on aerial photos using ground control 28
Alexander Vasilevsky and Burton L. Essex

Estimating d.b.h. from stump dimensions 30
Gerhard Raile

ERRORS IN SAMPLING PLANS BASED ON WALD'S SEQUENTIAL PROBABILITY RATIO TEST

Gary W. Fowler, *Associate Professor of Biometrics, School of Natural Resources, University of Michigan, Ann Arbor, Michigan*

Various sequential sampling plans based on Wald's Sequential Probability Ratio Test (SPRT) (Wald 1947, Wetherill 1966) have been developed for sampling forest populations. Such plans have been used to test hypotheses for decisionmaking and to classify populations. At least 27 plans have been developed to aid in monitoring insect populations or their damage.

Some plans were based on one SPRT to yield a two decision procedure such as control versus no control, while others were based on two SPRT's to yield a three decision procedure such as light versus medium versus heavy infestations. Because most sequential sampling plans in forestry have been applied to the field of entomology, this paper will emphasize entomological examples.

The sample size needed to make a decision to accept or reject a hypothesis for sequential sampling plans based on Wald's SPRT is a random variable. A decision to accept or reject a hypothesis or to continue sampling is made after each observation is taken, and observations are taken until enough evidence has been collected to make one of the terminating decisions. Such plans usually require only 40 to 60 percent as many observations as an equally reliable fixed sample size procedure. They are intuitively appealing in that few observations are needed to make a terminating decision when, for example, insect populations are sparse or abundant. Given the budget restraints faced today, sequential sampling plans should find wide applicability where we need to classify populations or compare populations with some standard for decisionmaking purposes and observations are time consuming, costly, and/or destructive. Such plans would also be useful when it is important to make a quick decision.

The first step in constructing a sequential sampling plan is to define the sampling unit and associated random variable of interest. The distribution of the random variable must then be determined. All of the plans developed to sample forest populations are based on either the binomial, negative binomial, normal, or Poisson distributions. For the normal and negative binomial distributions, the population variance σ^2 and the clumping parameter K, respectively, are assumed known, and if unknown must be estimated.

The second step is to set the class limits (e.g., economic thresholds or pest density levels), the simple null and alternative hypothesis parameter values of the underlying random variable, and the associated risk levels (probabilities of a Type I Error (α) and a Type II Error (β)). The gap between the two class limits (the interval between treatment and nontreatment thresholds) depends on the biology and behavior of the insect and its damage (Knight 1967; Waters 1955, 1974). The two class limits define three decision zones: the two terminating decisions or category classifications such as no control (acceptance of the null hypothesis) and control (acceptance of the alternative hypothesis), and the no decision zone (continue sampling).

Because there are two class limits or simple hypotheses that are used to construct a SPRT, two types of error can occur in decisionmaking:

(1) accepting the null hypothesis when the alternative hypothesis is true and (2) accepting the alternative hypothesis when the null hypothesis is true. The probabilities (risks) of these errors must be set in advance according to the seriousness of each error.

After the decision boundaries for a given SPRT have been developed given the underlying distribution and the class limits and associated risks, the operating characteristic (OC) and average sample number (ASN) properties of the test should be determined. Wald (1947) has developed OC and ASN equations to describe the properties of the test for all possible values of the random variable of interest. The OC equation or curve shows the probability of accepting the null hypothesis or lower classification, and the ASN equation or curve shows the average number of observations needed to make a terminating decision. The shapes of the OC and ASN curves depend upon the underlying distribution and class limits and associated risks (Waters 1974, Onsager 1976).

In all of the sequential sampling plans developed to sample forest populations, it is assumed that Wald's OC and ASN equations describe the actual OC and ASN functions of the plan, which means that the nominal values used to construct a SPRT are assumed to be the actual values. Wald's equations are developed on the assumption that a terminating decision is made as soon as a decision boundary is crossed. This assumption is not true because of the integer nature of the decision process of a SPRT, which results in overshooting of the decision boundaries when a terminating decision is made (fig. 1) (Wald 1947). Thus, Wald's equations are not accurate.

Wald's equations also assume that (1) only one observation is taken at each stage of the sequential process, (2) terminating decisions are possible after one observation has been taken, and (3) there is no upper limit to the number of observations taken before a terminating decision is made. Many forest researchers have modified the decision process of the SPRT by taking more than one observation at each stage of the sampling plan, not making a terminating decision until some minimum number of observations has been taken, and forcing a terminating decision to

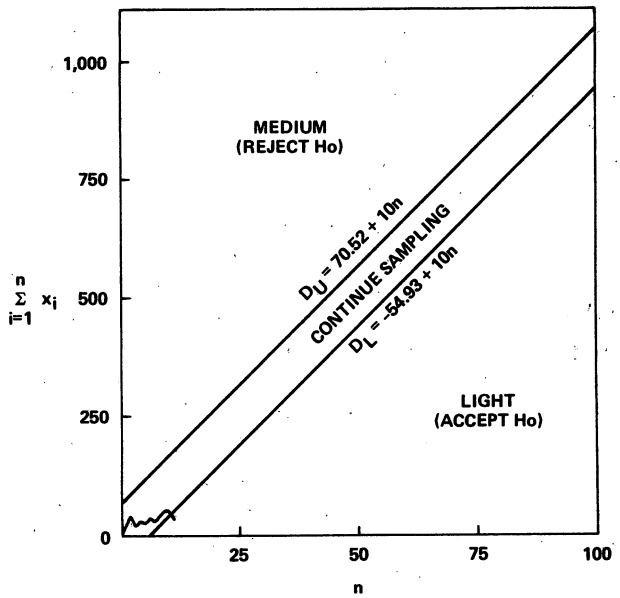

Figure 1. — *Acceptance (d_L) and rejection (d_U) decision boundaries for the lodgepole needleminer sequential sampling plan. Lines connecting points (.) show a sequential sample of 11 observations yielding a decision of light infestation. Notice overshooting of the lower decision boundary.*

be made at some maximum number of observations. Any of these modifications will, of course, affect the actual OC and ASN functions of a sampling plan. However, in all applications where one or more of these modifications are made, Wald's OC and ASN equations are still used to describe the properties of the sampling plan.

This paper examines (1) the errors inherent in Wald's OC and ASN equations due to overshooting of the decision boundaries and (2) the effects of the above modifications on the accuracy of Wald's equations for sequential sampling plans based on the normal distribution using Monte Carlo procedures.

WALD'S SPRT — NORMAL DISTRIBUTION

In forest sampling, Wald's SPRT is used to test the simple null hypothesis $H_0 : \theta = \theta_0$ against

the simple alternative hypothesis $H_1: \theta = \theta_1$ ($\theta_1 > \theta_0$), where θ is the test parameter of the distribution of the random variable X. The binomial distribution is used to describe X when X takes on one of two values (X = 1 for tree or plant or part of tree or plant infested and X = 0 for tree or plant or part of tree or plant not infested). The negative binomial, normal, or Poisson distributions are usually used to describe X when X is the number of insects per sampling unit. θ_0 and θ_1 define the class limits for the two decision categories — control or no control. The probability of a Type I Error (α) is the probability of rejecting H_0 when $\theta = \theta_0$, and the probability of a Type II Error (β) is the probability of rejecting H_1 when $\theta = \theta_1$. At the class limits, θ_0 and θ_1, the risk levels are set according to the seriousness of the two errors.

The two above simple hypotheses are used to develop the following decision rule: $H_0: \theta \leq \theta_0$ (no control) versus $H_1: \theta > \theta_0$ (control). The class limits, θ_0 and θ_1, are critical values of θ. If $\theta \geq \theta_1$ (the zone of rejection), protect against accepting H_0 by setting β at θ_1. If $\theta \leq \theta_0$ (the zone of acceptance), protect against rejecting H_0 by setting α at θ_0. If $\theta_0 < \theta < \theta_1$ (the zone of indifference), it does not matter what decision is made if θ is about halfway between θ_0 and θ_1 but becomes more important what decision is made as $\theta \rightarrow \theta_0$ and $\theta \rightarrow \theta_1$. This concern is expressed by the values of α and β set at θ_0 and θ_1, respectively. The values θ_0, θ_1, α, and β given the distribution of X describe a particular SPRT.

Decision Boundaries

The SPRT bases its decisons on a sequence of observations (x_1, x_2, . . .) from the given distribution of the random variable X. At each stage of the test, an observation is taken at random from the given distribution $f(x,\theta)$, and the probability ratio

$$R_n = \prod_{i=1}^{n} [\, f(x_i,\theta_1)/f(x_i,\theta_0)\,],$$

based on n observations taken up to and including the nth stage is calculated. At each stage one of the following decisions is made:

(1) If $R_n \geq A$, stop sampling and reject H_0.
(2) If $R_n \leq B$, stop sampling and accept H_0.
(3) If $B < R_n < A$, continue sampling.

$A \simeq (1-\beta)/\alpha$ and $B \simeq \beta/(1-\alpha)$. The approximate equalities are due to the fact that the number of observations is a discrete integer variable that causes overshooting of the decision boundaries before a terminating decision can be made for a SPRT (fig. 1). Observations are taken until one of the terminating decisions is made.

R_n can be simplified by taking the natural logarithm of each density function ratio in the product R_n, which yields $Z_n = \sum_{i=1}^{n} Z_i$ where $Z_i = \ln [\, f(x_i,\theta_1)/f(x_i,\theta_0)\,]$. The decision procedure is now

(1) If $Z_n \geq a$, stop sampling and reject H_0.
(2) If $Z_n \leq b$, stop sampling and accept H_0.
(3) If $b < Z_n < a$, continue sampling.

$a \simeq \ln A$ and $b \simeq \ln B$.

Z_n is usually converted to the statistic $\sum_{i=1}^{n} x_i$, which is easier to calculate, by setting $Z_n = a$ and $Z_n = b$ and solving for $\sum_{i=1}^{n} x_i$ to determine the upper rejection ($D_U = \sum_{i=1}^{n} x_i = h_2 + sn$) and lower acceptance ($D_L = \sum_{i=1}^{n} x_i = h_1 + sn$) boundaries, respectively. The decision boundaries are parallel straight lines with intercepts h_1 and h_2 and common slopes. The decision is now:

(1) If $\sum_{i=1}^{n} x_i \geq h_2 + sn$, stop sampling and reject H_0.
(2) If $\sum_{i=1}^{n} x_i \leq h_1 + sn$, stop sampling and accept H_0.
(3) If $h_1 + sn < \sum_{i=1}^{n} x_i < h_2 + sn$, continue sampling.

h_1, h_2, and s are calculated from θ_0, θ_1, α, and β. For the normal distribution,

$$f(x) = \frac{1}{(2\pi)^{1/2}\sigma} e^{-\frac{(x-\mu)^2}{2\sigma^2}}$$

$$h_1 = \frac{b\sigma^2}{\mu_1 - \mu_0}$$

$$h_2 = \frac{a\sigma^2}{\mu_1 - \mu_0}$$

$$s = \frac{\mu_1 + \mu_0}{2}$$

when the test parameter $\theta = \mu$, the mean of the distribution and the nontest parameter σ^2 is the variance of the distribution.

Once the density function f(x), θ_0, θ_1, α, and β are determined, the decision boundaries D_U and D_L are easily obtained from the probability ratio R_n. For the normal distribution, σ^2 is assumed known and if unknown must be estimated. Even though the decision boundaries are parallel straight lines, the probability of making a terminating decision is one. The class limits used for decisionmaking are in terms of the mean of the underlying distribution and are functions of the test parameter θ. For the normal distribution, the test parameter μ is the mean of the distribution. The equations for h_1, h_2, and s were summarized by Waters (1955) for the binomial, negative binomial, normal, and Poisson distributions. Talerico and Chapman (1970) developed a Fortran IV computer program (SEQUAN) to calculate h_1, h_2, and s and plot the decision boundaries for the four distributions above.

A sequential sampling plan based on the normal distribution will be used as an example throughout this paper. Stark (1952) developed a plan for classifying lodgepole needleminer (*Recurvaria milleri* Busck.) populations as light, medium, or heavy to make preliminary surveys of needleminer outbreak areas. The sampling unit was a branch tip including needles up to 5 years old, and the random variable was the number of live larvae per branch tip. It was determined that the number of live larvae per branch tip followed approximately a normal distribution, and the standard deviation σ was estimated to be 15.62. One of the SPRT's in the three decision (2SPRT) procedure was used to test whether insect infestations were light or medium. The class limits μ_0 and μ_1 were set at 5 and 15 larvae per branch tip, respectively, and α and β were set at 0.05 and 0.10, respectively.

The decision rule was to classify an infestation as light if $\mu \leq \mu_0 = 5$ and to classify it as heavy if $\mu > \mu_0 = 5$. If $\mu = 5$ for a specific needleminer population, the SPRT would indicate a medium infestation 1 out of 20 times when the infestation was light. If $\mu = 15$ for a specific needleminer population, the SPRT would indicate a light infestation 1 out of 10 times when the infestation was medium. Using the formulas for the normal distribution, h_1, h_2, and s were calculated to be -54.93, 70.52, and 10, respectively (fig. 1).

Wald's OC and ASN Equations

The OC function $L(\theta)$ is the probability of accepting H_0 as a function of θ. Wald's OC equation is $L(\theta) \simeq (A^{h(\theta)}-1)/A^{h(\theta)}-B^{h(\theta)})$ where A and B are as defined earlier and $h(\theta)$ is such that

$$\int_{-\infty}^{\infty} \left[\frac{f(x,\theta_1)}{f(x,\theta_0)}\right]^{h(\theta)} f(x,\theta)dx = 1$$

$$\sum_x \left[\frac{f(x,\theta_1)}{f(x,\theta_0)}\right]^{h(\theta)}$$

where x is a continuous or discrete variable, respectively, and $h(\theta) \neq 0$ (Wald 1947). To obtain points on the OC function, one of the above equations is solved for $h(\theta)$, θ is determined for various values of $h(\theta)$, and $L(\theta)$ is calculated. When $h(\theta) = 1$ and -1, $\theta = \theta_0$ and θ_1, respectively. For the case where $h(\theta) = 0$, $L(\theta) \simeq a/(a-b)$ (Wald 1947). For the normal distribution,

$$L(\mu) \simeq (A^{h(\mu)}-1)/(A^{h(\mu)}-B^{h(\mu)})$$

$$h(\mu) = \frac{\mu_1-\mu_0-2\mu}{\mu_1-\mu_0}$$

where $\theta = \mu$.

The ASN function $E_\theta(n)$ is the average number of observations needed to make a terminating decision. Wald's ASN equation is

$$E_\theta(n) \simeq E_\theta(Z_n)/E_\theta(Z) \text{ for } h(\theta) \neq 0$$

where $Z_n = \sum_{i=1}^{n} Z_i$ as defined earlier, $E_\theta(n) \simeq bL(\theta) + a[1-L(\theta)]$, and $E_\theta(Z) = E_\theta[\ln(f(x,\theta_1)/f(x,\theta_0))]$ (Wald 1947). To obtain points on the ASN function, $E_\theta(n)$ is calculated for several values of θ determined from $h(\theta)$ above. For the case where $h(\theta) = 0$, $E_\theta(n) \simeq ab/E_\theta(Z^2)$ (Wald 1947). For the normal distribution,

$$E_\mu(n) \simeq bL(\mu) + a[1-L(\mu)]$$

$$E_\mu(Z) = \left(\frac{\mu_1-\mu_0}{\sigma^2}\right)\left(\mu - \frac{\mu_1-\mu_0}{2}\right)$$

$$E_\mu(Z)^2 = \frac{(\mu_1-\mu_0)^2}{\sigma^2}$$

OC and ASN points for $h(\theta) = 4(-0.5)-4$ will usually describe the OC and ASN functions adequately. Formulas for Wald's OC and ASN equations for the four distributions discussed earlier were summarized by Waters (1955). Talerico and Chapman (1970) and I have developed Fortran IV computer programs to calculate OC and ASN points for selected values of $h(\theta)$. My program also calculates Monte Carlo OC and ASN points for selected values of $h(\theta)$. Wald's OC and ASN points for various values of $h(\mu)$ and μ are given in table 1 for the sampling plan presented earlier to classify populations of the lodgepole needleminer, and the resulting OC and ASN equations are shown in figure 2.

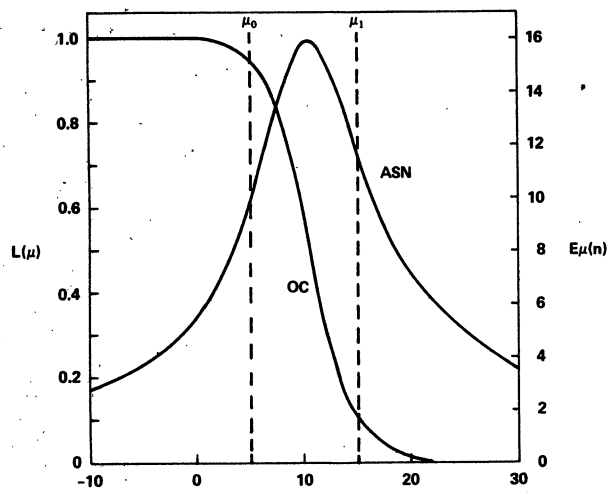

Figure 2. — *Wald's approximate OC ($L(\mu)$) and ASN ($E\mu(n)$) functions for the lodgepole needleminer sequential sampling plan. Notice that $L(\mu) = 1 - \alpha = 0.95$ at $\mu = \mu_0 = 5$ and $L(\mu) = \beta = 0.10$ at $\mu = \mu_1 = 15$.*

As mentioned earlier, Wald's OC and ASN equations, and associated nominal α and β, are only approximate in that they are based on the assumption that a terminating decision is made as soon as one of the decision boundaries is crossed. Because the number of observations is a discrete integer variable, overshooting of a decision boundary almost always occurs before a terminating decision is made. Wald (1947) states that the errors inherent in his equations due to overshooting are small if α and β are small (less than 0.05) and the class limits θ_0 and θ_1 are sufficiently close together. Because α and β are usually 0.10 (0.05 at the smallest) and the class limits are wide for most sampling plans in forestry, Wald's equations may not be good approximations to the unknown actual OC and ASN functions.

Sequential sampling plans require substantially fewer observations than equally-reliable fixed sample size procedures. For the lodgepole needleminer example, where $\mu_0 = 5$, $\mu_1 = 15$, $\sigma = 15.62$, $\alpha = 0.05$, and $\beta = 0.10$, approximately 21 observations are needed to yield $\alpha = 0.05$ @$\mu_0 = 5$ and $\beta = 0.10$ @$\mu_1 = 15$ for a fixed sample size Z - test. Compare this sample size with the ASN function for the sequential sampling plan (fig. 2). The advantage of the sequential sampling plan is clear. However, in comparing the two procedures, it must be remembered that Wald's equations are only approximate.

Table 1. — *Wald's Operating Characteristic ($L(\mu)$) and Average Sample Number ($E\mu(n)$) points for several values of $h(\mu)$ and μ for the lodgepole needleminer sequential sampling plan*

$h(\mu)$	μ	$L(\mu)$	$E_\mu(n)$	$h(\mu)$	μ	$L(\mu)$	$E_\mu(n)$
4	-10	1.000	2.75	-0.25	11.25	0.405	15.76
3	- 5	1.000	3.66	- .5	12.5	0.268	14.73
2	0	0.997	5.45	-1	15	0.100	11.60
1	5	0.950	9.73	-2	20	0.011	6.91
0.5	7.5	0.828	13.32	-3	25	0.001	4.69
0.25	8.75	0.711	14.96	-4	30	0.000	3.53
0	10	0.562	15.88				

THE ERRORS IN WALD'S OC AND ASN EQUATIONS

To investigate the effects of overshooting the decision boundaries of a given sequential sampling plan on the accuracy of Wald's OC and ASN equations, Monte Carlo simulation techniques were used to estimate the unknown actual OC and ASN functions. A distribution generator was developed to simulate taking observations at random from a normal distribution. The errors in Wald's equations were examined by comparing:

(1) Wald's nominal risk values (α and β) and associated average sample numbers (ASN) with Monte Carlo estimates of the actual risk values ($\hat{\alpha}$ and $\hat{\beta}$) and associated average sample numbers ($\hat{ASN}$) at class limits $\mu_0[h(\mu)=1]$ and $\mu_1[h(\mu)=-1]$ for various values of $\alpha=\beta$ and μ_0 and μ_1; and (2) Wald's OC and ASN equations and Monte Carlo estimates of the unknown actual OC and ASN functions for the lodgepole needleminer example.

A sensitivity analysis indicated that 5,000 and 1,000 samples from a normal distribution (trials or iterations) yielded adequate accuracy for the Monte Carlo $\hat{OC}$ and $\hat{ASN}$ values at $h(\mu)=\pm 1$ and $h(\mu)\neq\pm 1$, respectively. Unless otherwise stated, that many iterations were used. Any desired degree of accuracy can be obtained but the cost increases with the number of iterations. Throughout the discussion, OC and ASN refer to Wald's equations, $\hat{OC}$ and $\hat{ASN}$ refer to Monte Carlo functions, $SD_{\hat{OC}}=[\hat{OC}(1-\hat{OC})/\#trials-1]^{1/2}$ is the standard deviation of the $\hat{OC}$ value, $SE_{\hat{ASN}}$ is the standard error of the $\hat{ASN}$ value, and $RE_{ASN}=(ASN-\hat{ASN})/\hat{ASN}$ is the estimated error of Wald's ASN value.

The Pattern of Errors

To establish if there are any trends in the errors inherent in Wald's equations, Wald and Monte Carlo OC and ASN values at $h(\mu)=\pm 1$ were compared for $\alpha=\beta=0.05$, 0.10, and 0.20 and $\delta_1=0.1$, 0.25, 0.5, 1, 2, and 3 (tables 2 and 3). $\delta_1=(\mu_1-\mu_0)/\sigma$ is the noncentrality parameter of the standardized normal distribution.

Table 2. — *Comparison of Wald's and Monte Carlo values of α and β at $h(\mu)=\pm 1$ for several values of δ_1 and $\alpha=\beta$ for the normal distribution*

δ_1	$\alpha=\beta$								
	0.05			0.10			0.20		
	$\hat{\alpha}$	$SD_{\hat{\alpha}}$	RE_{α}	$\hat{\alpha}$	$SD_{\hat{\alpha}}$	RE_{α}	$\hat{\alpha}$	$SD_{\hat{\alpha}}$	RE_{α}
0.1	0.047	0.0015	0.064	0.093	0.0021	0.075	0.192	0.0020	0.042
.25	.046	.0010	.087	.088	.0014	.136	.177	.0019	.130
.5	.037	.0009	.351	.077	.0013	.299	.156	.0018	.282
1	.028	.0008	.786	.057	.0012	.915	.123	.0016	.626
2	.016	.0006	2.12	.031	.0009	2.23	.064	.0012	2.12
3	.008	.0004	5.25	.016	.0006	5.25	.028	.0008	6.14

Table 3. — *Comparison of Wald's and Monte Carlo values of Average Sample Number (ASN) at $h(\mu)=\pm 1$ for several values of δ_1 and $\alpha=\beta$ for the normal distribution*

δ_1	$\alpha=\beta$											
	0.05				0.10				0.20			
	ASN	$\hat{ASN}$	$SE_{\hat{ASN}}$	RE_{ASN}	ASN	$\hat{ASN}$	$SE_{\hat{ASN}}$	RE_{ASN}	ASN	$\hat{ASN}$	$SE_{\hat{ASN}}$	RE_{ASN}
0.1	530.0	541.5	3.87	-0.021	351.6	367.5	1.97	-0.043	166.4	179.1	0.71	-0.074
.25	84.8	90.9	.32	- .067	56.2	62.2	.23	- .096	26.6	31.8	.12	- .164
.5	21.2	24.2	.08	- .124	14.1	17.1	.06	- .175	6.6	9.5	.04	- .305
1	5.3	7.0	.023	- .243	3.5	5.2	.018	- .327	1.7	3.2	.012	- .469
2	1.3	2.3	.007	- .435	.9	1.9	.006	- .526	.4	1.5	.004	- .733
3	.6	1.4	.003	- .571	.4	1.2	.003	- .667	.2	1.1	.002	- .818

The OC value at $h(\mu) = 1$ is $1-\alpha$, and the OC value at $h(\mu) = -1$ is β. Because $\alpha = \beta$ and the normal distribution is symmetrical, the Monte Carlo results at $h(\mu) = \pm 1$ were pooled. The results were based on 40,000 iterations for each combination of $\alpha = \beta$ and δ_1 except for values at $\alpha = \beta = 0.05$ and 0.10 and $\delta_1 = 0.10$, which were based on 20,000 iterations.

Results showed that $\hat{\alpha}$ and $\hat{\beta}$ were always less than α and β and $\hat{ASN}$ values were always larger than ASN values. The errors in Wald's equations increased as δ_1 increased. The errors in Wald's ASN equation increased as $\alpha = \beta$ increased with no apparent trend for the errors in Wald's OC equation. The errors in Wald's equations are large for high values of δ_1.

An Example

Wald's OC and ASN equations were compared with Monte Carlo $\hat{OC}$ and $\hat{ASN}$ functions for several values of $h(\mu)$ for the lodgepole needleminer sequential sampling plan with $\mu_0 = 5$, $\mu_1 = 15$, $\sigma = 15.62$, $\alpha = 0.05$ and $\beta = 0.10$ (table 4, figs. 3 and 4). In general, Wald's OC equation underestimated the actual OC function near μ_0 ($\mu < 10$) and overestimated it near μ_1 ($\mu \geq 10$) with $\hat{\alpha} = 0.036$ and $\hat{\beta} = 0.073$. Wald's ASN equation always underestimated the actual ASN function; the largest error was near $h(\mu) = 0$ where ASN reaches a maximum. The errors in Wald's equations were moderately serious for this example even though $\delta_1 = 0.64$ is not large.

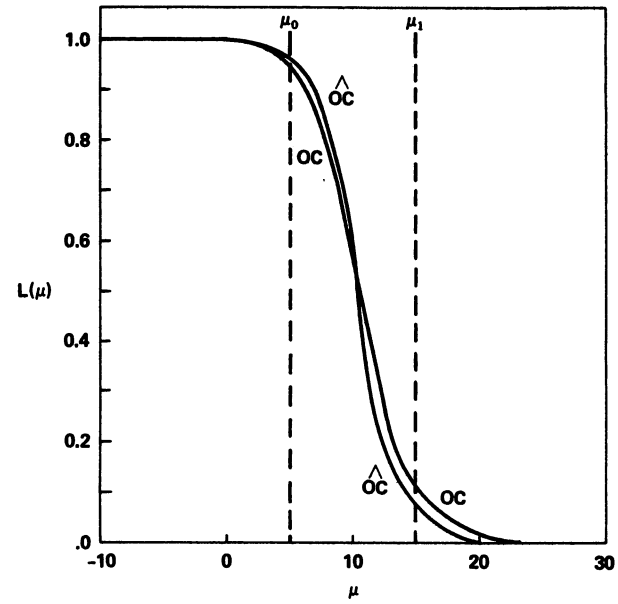

Figure 3. — *Comparison of Wald's and the Monte Carlo Operating Characteristic (OC) functions for the lodgepole needleminer sequential sampling plan (table 4).*

Table 4. — *Comparison of Wald's and Monte Carlo Operating Characteristic (OC) and Average Sample Number (ASN) values for several values of $h(\mu)$ and μ for the lodgepole needleminer sequential sampling plan ($\mu_0 = 5$, $\mu_1 = 15$, $\sigma = 15.62$, $\alpha = 0.05$, and $\beta = 0.10$)*

		OC				ASN						
$h(\mu)$	μ	OC	$\hat{OC}$	$SD_{\hat{OC}}$	$OC-\hat{OC}$	ASN	$\hat{ASN}$	$SE_{\hat{ASN}}$	RE_{ASN}	R_{DSN}[1]	[1]$\hat{\gamma}_1$	[1]$\hat{\gamma}_2$
4	-10	1.000	1.000			2.75	3.40	0.04	-0.19	1-11	1.25	2.61
3	- 5	1.000	1.000			3.66	4.57	.07	- .20	1-17	1.64	4.11
2	0	0.997	1.000		-0.003	5.45	6.66	.13	- .18	1-33	1.70	4.02
1	5	.950	0.964	0.003	- .014	9.73	11.84	.12	- .18	1-74	1.84	4.98
0.5	7.5	.828	.866	.011	- .038	13.32	17.11	.44	- .22	1-80	1.88	4.89
.25	8.75	.711	.749	.014	- .038	14.96	19.11	.50	- .22	1-97	1.99	5.52
0	10	.562	.557	.016	+ .005	15.88	21.58	.56	- .26	1-95	1.74	3.88
- .25	11.25	.405	.392	.015	+ .013	15.76	19.73	.48	- .20	1-92	2.05	7.22
- .5	12.5	.268	.211	.013	+ .057	14.73	19.20	.48	- .23	1-100	2.12	6.26
-1	15	.100	.073	.004	+ .027	11.60	14.35	.14	- .19	1-94	1.78	4.63
-2	20	.011	.001	.001	+ .10	6.91	8.17	.14	- .15	1-35	1.61	3.78
-3	25	.001	.001	.001		4.69	5.45	.07	- .14	1-18	1.29	2.86
-4	30	.000	.000			3.53	4.23	.05	- .16	1-13	1.20	2.87

[1]R_{DSN}=range of the decisive sample number; $\hat{\gamma}_1$=skewness coefficient; $\hat{\gamma}_2$= kurtosis coefficient.

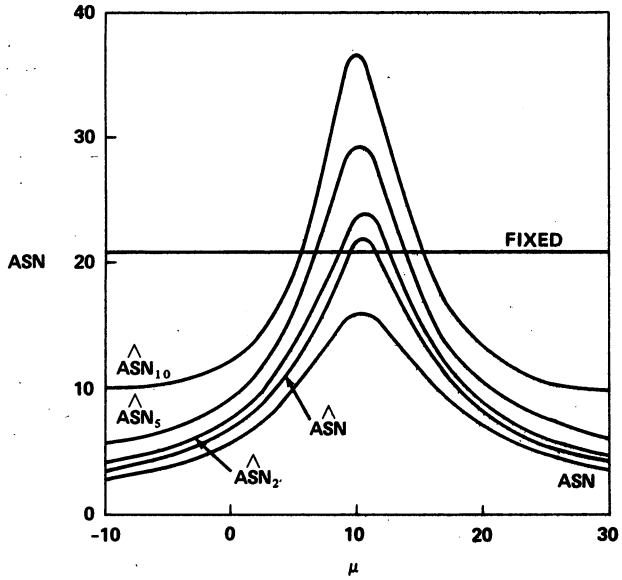

Figure 4. — *Comparison of Monte Carlo Average Sample Number ($\hat{ASN}$) functions for sequential sampling plans with $\mu_0 = 5$, $\mu_1 = 15$, $\sigma = 15.62$, $\alpha = 0.05$, and $\beta = 0.10$, for numbers of observations taken at each stage of the plan equal to 1, 2, 5, and 10. The ASN function for the fixed sample size plan with equal reliability is also shown.*

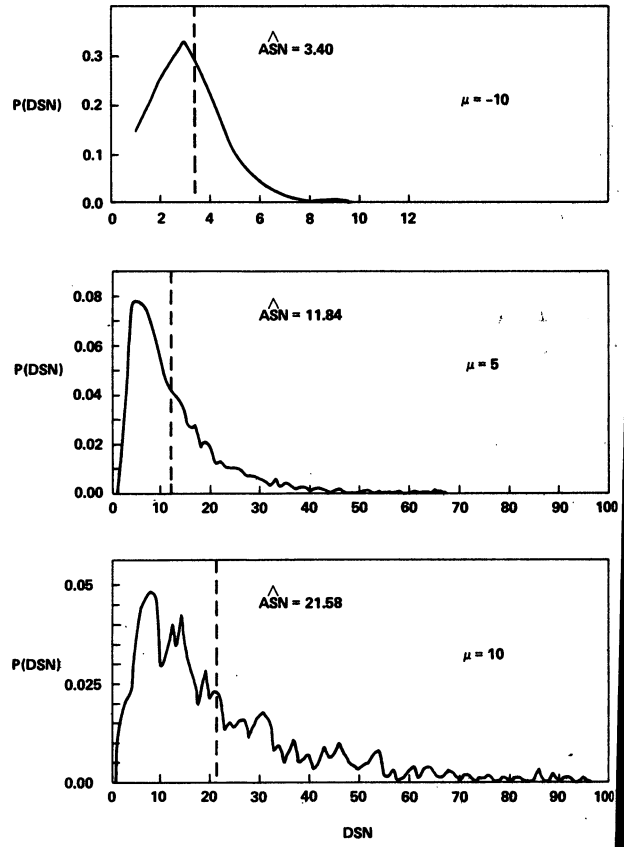

Figure 5. — *Empirical distributions of the Decisive Sample Number (DSN) for three values of μ for Wald's Sequential Probability Ratio Test (SPRT) with $\alpha = 0.05$ and $\beta = 0.10$. The dashed line shows the mean Average Sample Number ($\hat{ASN}$) for each DSN distribution.*

It must be remembered that the ASN value is the average number of observations needed to make a terminating decision. The number of observations needed to make a terminating decision for one sample is a random variable called the decisive sample number (DSN), and the ASN is the mean of this random variable. The seriousness in the errors of Wald's equations can be better shown by looking at the distribution of the DSN (table 4, fig. 5). The distributions of DSN are skewed to the right; the skewness increases as $\hat{ASN}$ increases. The number of observations needed to make a decision for a particular sequential sample can be much larger than $\hat{ASN}$.

Procedure to Obtain More Accurate OC and ASN Functions

Monte Carlo results for the normal distribution showed that the errors inherent in Wald's OC and ASN equations can be large and are a function of the difference between the pest density levels or class limits ($\delta_1 = (\mu_1 - \mu_0)/\sigma$) and associated error probabilities used to construct a given sequential sampling plan. The practical consequences of these errors are (1) the actual error probabilities can be smaller than the nominal error probabilities used to build the sampling plan, and (2) more field observations are made than necessary. If sampling is destructive, time consuming, expensive, and/or early decisions are desirable, the consequences of these errors can be severe. Monte Carlo procedures should be used to determine if these errors are serious for a given sampling plan, and if they are, new sequential sampling plans should be developed to yield actual error probabilities, and resulting OC and ASN functions, approximately equal to the nominal ones desired.

In developing a sequential sampling plan, Monte Carlo $\hat{OC}$ and $\hat{ASN}$ functions should be obtained for the decision boundaries based on the nominal values of α and β. If $\hat{\alpha}$ and $\hat{\beta}$ are close enough to α and β and Wald's and the Monte Carlo OC and ASN functions are similar, the Monte Carlo functions should be used to describe the operation of the sequential sampling plan. If the errors associated with Wald's equations are serious, new nominal values of $\alpha(\alpha')$ and $\beta(\beta')$ should be determined to yield new Monte Carlo estimates $\hat{\alpha}'$ and $\hat{\beta}'$ that are approximately equal to the desired (old nominal values) of α and β. Monte Carlo $\hat{OC}'$ and $\hat{ASN}'$ functions can then be obtained for the new sequential sampling plan based on the new nominal error probabilities α' and β'. If $\hat{\alpha}'$ and $\hat{\beta}'$ are not close enough to α and β, as many iterations of this procedure as are necessary to yield the desired Monte Carlo values of $\hat{\alpha}'$ and $\hat{\beta}'$ should be used. Usually one or two iterations will be sufficient.

Considering the lodgepole needleminer problem, if the difference between the Monte Carlo $\hat{OC}$ and $\hat{ASN}$ functions with $\hat{\alpha} = 0.036$ and $\hat{\beta} = 0.073$ and Wald's OC and ASN functions with $\alpha = 0.05$ and $\beta = 0.10$ (table 4, figs. 3 and 4) are not considered important, then the Monte Carlo $\hat{OC}$ and $\hat{ASN}$ functions should be used to describe the operation of the original sampling plan based on $\alpha = 0.05$ and $\beta = 0.10$.

If the errors in Wald's equations are considered serious, a new sampling plan should be constructed. $\hat{\alpha}$ and $\hat{\beta}$ were determined to be 0.035 and 0.072, respectively, based on 20,000 iterations each. To determine new nominal values α' and β' that yield new Monte Carlo values $\hat{\alpha}'$ and $\hat{\beta}'$ that are approximately equal to the desired old nominal values α and β, $\alpha' = (\alpha/\hat{\alpha})\alpha = \alpha^2/\hat{\alpha}$ and $\beta' = (\beta/\hat{\beta})\beta = \beta^2/\hat{\beta}$. For our example, $\alpha' = (0.05)^2/0.035 = 0.0714$ and $\beta' = (0.10)^2/0.072 = 0.1389$. Using these new nominal values, new decision boundaries can be developed for a new sequential sampling plan and Monte Carlo $\hat{OC}'$ and $\hat{ASN}'$ functions can be obtained (table 5). $\hat{\alpha}' = 0.051$ with $SD_{\hat{\alpha}'} = 0.003$, and $\hat{\beta}' = 0.097$ with $SD_{\hat{\beta}'} = 0.004$. Notice the difference between the $\hat{ASN}'$ values for the new sampling plan and the $\hat{ASN}$ values for the old sampling plan (table 4). Also, compare the empirical distribution of DSN' of the new sampling plan (table 5, fig. 6) with the empirical distributions of DSN for the old sampling plan (table 4, fig. 5) for $\mu = -10$, 5, and 10.

Notice the close agreement between $\hat{OC}$ and $\hat{ASN}'$ of the new plan and OC and ASN of the old plan. A comparison of the $\hat{ASN}'$ function of the new sampling plan ($\hat{\alpha}' = 0.051$, $\hat{\beta}' = 0.097$) (table 5), which is closely approximated by the ASN function of the old sampling plan (fig. 4), with the ASN function of the fixed sample size Z - test sampling plan (FIXED, $\alpha = 0.05$, $\beta = 0.10$, $n = (Z_\alpha + Z_\beta)^2/\delta_1^2 \simeq 21$) is more valid than the comparison with the $\hat{ASN}$ function of the old sampling plan ($\hat{\alpha} = 0.035$, $\hat{\beta} = 0.072$). This comparison is also more in favor of the sequential procedure.

Table 5. — *Monte Carlo Operating Characteristic (OC) and Average Sample Number (ASN) values for several values of $h(\mu)$ and μ for the lodgepole needleminer sequential sampling plan ($\mu_0 = 5$, $\mu_1 = 15$, $\sigma = 15.62$, $\alpha' = 0.0714$, and $\beta' = 0.1389$)*

$h(\mu)$	μ	OC		ASN					
		$\hat{OC}'$	$SD_{\hat{OC}'}$	$\hat{ASN}'$	$SE_{\hat{ASN}'}$	$SD_{DSN'}$	$R_{DSN'}$	$\hat{\gamma}_1'$	$\hat{\gamma}_2'$
4	-10	1.000		3.07	0.04	1.36	1-9	1.16	1.76
3	- 5	1.000		4.01	.06	2.25	1-15	1.48	3.48
2	0	0.993	0.002	5.70	.11	3.99	1-23	1.43	2.41
1	5	.949	.003	9.97	.10	8.66	1-63	1.77	4.24
0.5	7.5	.818	.012	14.07	.38	13.82	1-75	2.34	8.90
.25	8.75	.726	.014	14.51	.38	15.76	1-91	2.21	8.09
0	10	.568	.016	16.40	.42	17.57	1-91	1.88	5.38
- .25	11.25	.407	.016	16.61	.40	15.25	1-88	1.71	3.75
- .5	12.5	.255	.014	14.68	.35	15.28	1-79	1.65	3.32
-1	15	.097	.004	11.92	.12	9.83	1-67	1.75	4.30
-2	20	.012	.003	7.16	.12	4.38	1-25	1.38	2.45
-3	25	.001	.001	4.81	.07	2.35	1-18	1.40	3.26
-4	30	.000		3.70	.05	1.55	1-13	1.40	3.61

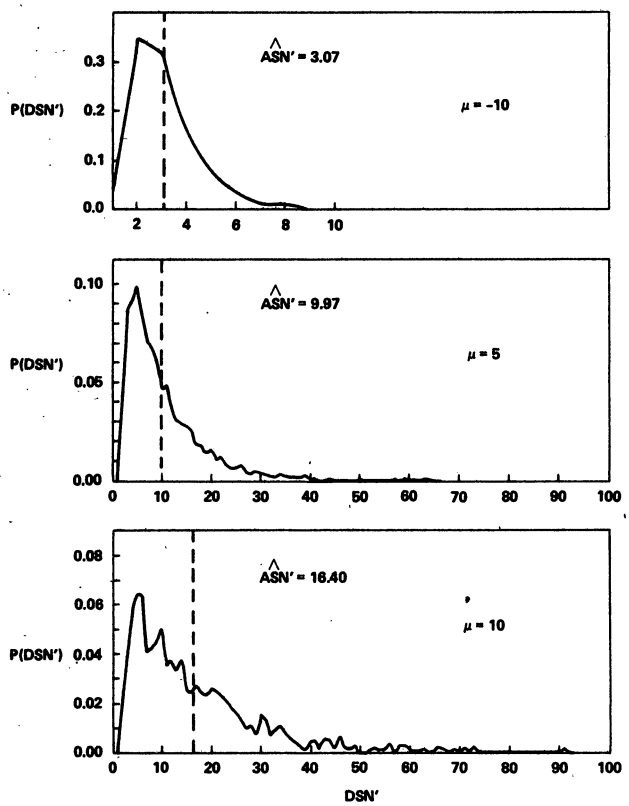

Figure 6. — *Empirical distributions of the Decisive Sample Number (DSN') for three values of μ for Wald's Sequential Probability Ratio Test (SPRT) with α' = 0.0714 and β' = 0.1389. The dashed line shows the mean Average Sample Number (ÂSN) for each DSN distribution.*

MODIFICATIONS OF WALD'S SPRT

Many forest researchers (Cole 1960; Connola *et al.* 1959; Ives 1954; Ives and Prentice 1958; Knight 1960a, b; Tostowaryk and McLeod 1972) have modified the decision process of sequential sampling plans based on Wald's SPRT by taking more than one observation at each stage of the plan, not making a terminating decision until some minimum number of observations has been taken, and/or forcing a terminating decision to be made at some maximum number of observations. These deviations from the assumptions of Wald's SPRT will, of course, affect the actual OC and ASN functions of the modified sampling plan. However, in all forest applications where one or more of these modifications are made, Wald's OC and ASN equations are still used to describe the properties of the modified sampling plan.

To investigate the effects of these modifications on the accuracy of Wald's equations in describing the actual OC and ASN functions of the modified sampling plans, Monte Carlo $\hat{OC}$ and $\hat{ASN}$ functions were obtained for the following sampling plans for the lodgepole needleminer example ($\mu_0 = 5$, $\mu_1 = 15$, $\sigma = 15.62$, $\alpha = 0.05$, $\beta = 0.10$):

(1) Wald's SPRT with no modifications.
(2) Wald's SPRT with 2, 5, and 10 observations taken at each stage.
(3) Wald's SPRT truncated at 10, 16, and 21 observations.
(4) Wald's SPRT with terminating decisions first possible at a minimum of three and five observations (minimum points).
(5) Wald's SPRT with (a) a minimum point of 5, (b) a truncation point of 10, (c) a minimum point of 5 and a truncation point of 10, and (d) a minimum point of 5, a truncation point of 10, and 5 observations at each stage.

To obtain $\hat{OC}$ and $\hat{ASN}$ values, 5,000 and 1,000 iterations were used for each sampling plan at $h(\mu) = \pm 1$ and $h(\mu) \neq \pm 1$, respectively.

Two to 10 observations taken at each stage represent the range encounter in forestry sampling plans. A truncation point of 16 was obtained using Water's (1974) suggestion of using the maximum of Wald's ASN function as the maximum point, and a truncation point of 21 was obtained from Wald's (1947) rule for truncation, which is to use the sample size of the equally reliable ($\alpha = 0.05$, $\beta = 0.10$) fixed sample size Z - test as the maximum point. A truncation point of 10 is approximately the average truncation point encountered in forestry sampling plans — Wald's ASN value at $h(\mu) = 1$. If a terminating decision has not been made when the truncation point is reached, the average of the acceptance and rejection value at that stage is used as the decision point. The largest minimum point used in forestry sampling plans is 5.

Monte Carlo results were obtained with the same starting seed value for the random number generator for sampling plans with number of observations equal to 1, 2, 5, and 10; truncation points of 10, 16, and 21; and a minimum point of 5. Monte Carlo results were also obtained for sampling plans with number of observations equal to 1 and a minimum point of 5 using a different starting seed. This was done to reduce Monte Carlo variability in comparing the different modified sampling plans and to show Monte Carlo variability in the case of the $\hat{OC}$ and $\hat{ASN}$ values for Wald's SPRT (number of observations = 1) (table 6).

The Monte Carlo results showed that $\hat{\alpha}$ and $\hat{\beta}$ become smaller and the associated $\hat{ASN}$ values at $h(\mu) = \pm 1$ becomes larger as the number of observations taken at each stage, truncation point, or minimum point increase (table 6). These trends are distinct for the range of number of observations taken at each stage and the truncation points considered and slight for the range of minimum points considered. The Monte Carlo variability in estimating $\hat{\alpha}$ and $\hat{\beta}$ was larger than the Monte Carlo variability in estimating the associated $\hat{ASN}$ values at $h(\mu) = \pm 1$ for Wald's SPRT with no modifications.

The $\hat{ASN}$ functions increased substantially as the number of observations at each stage increased, and the $\hat{ASN}$ functions decreased substantially as the truncation point decreased (figs. 4 and 7). Wald's SPRT with Wald's truncation point (21) yielded as $\hat{ASN}$ function closer to the $\hat{ASN}$ function of Wald's unmodified SPRT than both Wald's SPRT with Water's truncation point (16) or the average truncation point used in forestry examples (10). However, the $\hat{ASN}$ function is still larger than the $\hat{ASN}_{21}$ function for $5 \leq \mu \leq 15$.

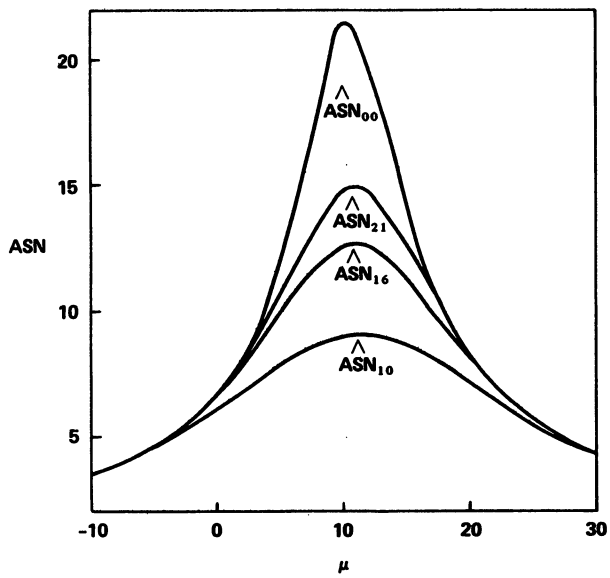

Figure 7. — *Comparison of Monte Carlo Average Sample Number ($\hat{ASN}$) functions for sequential sampling plans ($\mu_0 = 5$, $\mu_1 = 15$, $\sigma = 15.62$, $\alpha = 0.05$, and $\beta = 0.10$) for truncation points of $N = 10, 16, 21$, and ∞.*

Table 6. — *Comparison of Monte Carlo values of α and β and Average Sample Numbers (ASN's) at $h(\mu) = \pm 1$ for sequential sampling plans ($\mu_0 = 5$, $\mu_1 = 15$, $\sigma = 15.62$, $\alpha = 0.05$, and $\beta = 0.10$) for various numbers of observations taken at each stage of the plan, various truncation points, or various minimum number of observations*

$h(\mu)$	$L(\mu)$	Number of observations					Truncation points			Minimum number of observations	
		1	1[1]	2	5	10	10	16	21	3[1]	5
1	$\hat{\alpha}$[2]	0.036	0.032	0.031	0.023	0.020	0.123	0.077	0.061	0.032	0.035
	$\hat{ASN}$	11.84	11.86	13.19	15.54	18.84	7.86	9.87	10.74	11.89	12.22
-1	$\hat{\beta}$[3]	.073	.071	.066	.049	.031	.202	.140	.111	.071	.069
	$\hat{ASN}$	14.35	14.27	15.22	17.60	21.25	8.62	11.28	12.53	14.28	14.58

[1]Based on a different Monte Carlo run than the other Operating Characteristic ($\hat{OC}$) and $\hat{ASN}$ values.
[2]$\hat{\alpha} = 1 - \hat{OC} = 1 - L(\mu)$ for $h(\mu) = 1$.
[3]$\hat{\beta} = \hat{OC} = L(\mu)$ for $h(\mu) = -1$.

Monte Carlo results were obtained with the same starting seed value for Wald's unmodified SPRT and for Wald's SPRT with one observation at each stage and (a) a minimum point of 3, (b) a truncation point of 10, and (c) a minimum point of 3 and a truncation point of 10 (table 7). Monte Carlo results were also obtained with a different starting seed value for Wald's unmodified SPRT and for Wald's SPRT with one observation taken at each stage and (a) a minimum point of 5, (b) a truncation point of 10, and (c) a minimum point of 5 and a truncation point of 10. Monte Carlo results were also obtained for Wald's SPRT with 5 observations taken at each stage, a minimum point of 5, and a truncation point of 10.

The Monte Carlo results showed that in comparison to Wald's unmodified SPRT:

(1) a minimum point decreased $\hat{\alpha}$ and $\hat{\beta}$ and increased the associated $\hat{ASN}$ values at $h(\mu) = \pm 1$ with these effects increasing slightly as the minimum point increased from 3 to 5;

(2) a truncation point increased $\hat{\alpha}$ to $\hat{\beta}$ and decreased the associated $\hat{ASN}$ values at $h(\mu) = \pm 1$;

(3) the effects of a minimum and a truncation point above and beyond the effects of a truncation point are none to small decreases in $\hat{\alpha}$ and $\hat{\beta}$ and small increases in the associated $\hat{ASN}$ values at $h(\mu) = \pm$ with these effects increasing slightly the minimum point increased from 3 to

(4) the effects of more than one observatio each stage above and beyond the effect a truncation and minimum point are creases in $\hat{\alpha}$ and $\hat{\beta}$ and increases in the sociated $\hat{ASN}$ values at $h(\mu) = \pm 1$.

The three modifications of Wald's SPRT sidered in this paper definitely affect the ac racy of Wald's equations in describing the act OC and ASN equations of the modified sampl plans. The size of the errors in Wald's equati depends on how far these modifications dev from the assumptions of Wald's SPRT and w combination of modifications are used.

CONCLUDING REMARKS

Assuming a normal distribution, a compari of Wald's and Monte Carlo OC and ASN fu tions indicated that the errors inherent in Wal equations can be serious. The practical co quences of these errors are: (1) the actual e probabilities can be smaller than the nomi error probabilities used to build the sampl plan, and (2) more observations are usu taken in the field than necessary. These er

Table 7. — *Comparison of Monte Carlo values of α and β and Average Sample Numbers (ASN's) at $h(\mu) = \pm 1$ for sequential sampling plans ($\mu_0 = 5$, $\mu_1 = 15$, $\sigma = 15.62$, $\alpha = 0.05$, and $\beta = 0.10$) for two Monte Carlo runs with various combinations of numbers of observations taken at each stage of the plan, truncation points, and minimum number of observations*

Run number		1					2			
No. of observations		1					1			5
Minimum[1]		1	3	1	3	1	5	1	5	
Truncation point[1]		∞		10		∞	∞	10		
$h(\mu) = 1$	$\hat{\alpha}$[2]	.032	.032	.115	.115	.036	.035	.123	.123	.119
	$\hat{ASN}$	11.86	11.89	7.84	7.88	11.84	12.22	7.86	8.19	9.01
$h(\mu) = -1$	$\hat{\beta}$[3]	.071	.071	.194	.194	.073	.069	.202	.200	.196
	$\hat{ASN}$	14.27	14.28	8.64	8.65	14.35	14.58	8.62	8.78	9.45

[1]A minimum of 1 indicates no minimum point, a truncation point of ∞ indicates no truncation point, and a minimum of 1 and a truncation point of ∞ indicates an unmodified sequential sampling plan.

[2]$\hat{\alpha} = 1 - \hat{OC} = 1 - L(\mu)$ for $h(\mu) = 1$.

[3]$\hat{\beta} = \hat{OC} = L(\mu)$ for $h(\mu) = -1$.

increase as the difference between the class limits ($\delta_1 = (\mu_1 - \mu_0)/\sigma$) and associated error probabilities (α and β) used to build a sequential sampling plan increase. Similar results have been obtained for the binomial, negative binomial, and Poisson distributions.

Also assuming a normal distribution, Monte Carlo results indicate that any of the above modifications will affect the actual OC and ASN functions of the sequential sampling plan and thus decrease the accuracy of Wald's equations in describing these actual functions. The practical consequences of these modifications are (1) the actual error probabilities decrease and the ASN function increases as the number of observations taken at each stage increases, (2) the actual error probabilities increase and the ASN function decreases as the truncation point decreases, and (3) the actual error probabilities decrease and the ASN function increases as the minimum point increases. Similar results would be obtained for the binomial, negative binomial, and Poisson distributions.

Regardless of what distribution and whether no or any combination of the above modifications were used in developing a sampling plan based on Wald's SPRT, I strongly suggest that Monte Carlo $\hat{OC}$ and $\hat{ASN}$ functions be obtained for the decision boundaries of the original SPRT. If $\hat{\alpha}$, $\hat{\beta}$, and the Monte Carlo functions are considered to be not seriously divergent from α, β, and Wald's equations, then the Monte Carlo functions should be used to describe the actual functions of the original sampling plan.

If, on the other hand, the differences between Wald's and Monte Carlo results are substantial, a new sampling plan should be developed using the procedure presented in this paper so that the Monte Carlo values $\hat{\alpha}'$ and $\hat{\beta}'$ of the new plan are approximately equal to the nominal values α and β of the old plan. Monte Carlo $\hat{OC}'$ and $\hat{ASN}'$ functions should then be obtained for the decision boundaries of the new plan and used to describe the actual functions.

Given the budget available, the time and cost of taking observations, whether sampling is destructive or not, and the importance of early decisions, the forest researcher will have to decide whether to use fixed sample size or sequential sampling plans. If a sequential sampling plan is used, the forest researcher then must decide whether to construct the new or old sequential sampling plan and associated Monte Carlo $\hat{OC}$ and $\hat{ASN}$ functions. The only fair comparison is between the fixed sample size and the new sequential sampling plan. For either sequential sampling plan, the cost of obtaining $\hat{OC}$ and $\hat{ASN}$ functions is inexpensive.

LITERATURE CITED

Cole, Walter E. 1960. Sequential sampling in spruce budworm control projects. For. Sci. 6:51-59.

Connola, D. P., W. E. Waters, and E. R. Nason. 1959. A sequential sampling plan for red-pine sawfly Neodiprion nanulus *Schedl. J. Econ. Entomol. 52:600-602.*

Ives, W. G. H. 1954. Sequential sampling of insect populations. For. Chron. 30:287-291.

Ives, W. G. H., and R. M. Prentice. 1958. A sequential sampling technique for surveys of the larch sawfly. Can. Entomol. 90:331-338.

Knight, Fred B. 1960a. Sequential sampling of Black Hills beetle populations. U.S. Dep. Agric. For. Serv. Res. Note RM-48, 8 p. Rocky Mountain For. and Range Exp. Stn., Ft. Collins, Colorado.

Knight, Fred B. 1960b. Sequential sampling of Engelmann spruce beetle infestations in standing trees. U.S. Dep. Agric. For. Serv. Res. Note RM-47, 4 p. Rocky Mountain For. and Range Exp. Stn., Ft. Collins, Colorado.

Stark, Ronald W. 1952. Sequential sampling of the lodgepole needleminer. For. Chron. 28:57-60.

Talerico, Robert L., and Roger C. Chapman. 1970. Sequan: a computer program for sequential analysis. U.S. Dep. Agric. For. Serv. Res. Note NE-116, 6 p. Northeast. For. Exp. Stn., Upper Darby, Pennsylvania.

Tostowaryk, W., and J. M. McLeod. 1972. Sequential sampling for egg clusters of the swain jack pine sawfly, Neodiprion swainei *(Hymenoptera: diprionidae). Can. Entomol. 104:1343-1347.*

Wald, Abraham. 1947. Sequential analysis. 212 p. John Wiley and Sons, Inc., New York.

Waters, William E. 1955. Sequential sampling in forest insect surveys. For. Sci. 1:68-79.

Waters, William E. 1974. Sequential sampling applied to forest insect surveys. IUFRO/SAF/SUNY Symposium on Monitoring Forest Environment through Successive Sampling. 22 p.

Wetherill, G. Barrie. 1966. Sequential methods in statistics. 216 p. John Wiley and Sons, Inc., New York.

A COMPARISON OF TWO METHODS USED TO ESTIMATE STAND STOCKING IN UPLAND CENTRAL HARDWOODS

Robert Rogers, *Research Forester, Columbia, Missouri*

The term stand stocking used in this paper refers to the density of trees in a stand expressed by the formula given by Gingrich (1967)[1] :

Stand Stocking Percent (SSP) =
$(-0.0507N + 0.1698\,\Sigma D + 0.0317\,\Sigma D^2)/10$

where
N = number of trees per acre
ΣD = sum of their individual diameters
ΣD^2 = sum of the squares of their diameters.

Each tree in the stand must be tallied and measured to derive stocking percent using the above equation. This process is time consuming, so sampling methods are used to estimate the quantities needed for the stocking equation.

One sampling method, which I call "variable plus fixed area sampling" (F), provides an estimate of basal area from the variable area plot and an estimate of the number of trees from the fixed area plot with origin in common with the point.

Typically, the fixed area plot is circular with 1/20 acre area. Thus

BA = basal area/acre = BAF x k = basal area factor x point sample tree count
n = no. of trees/acre = fixed plot tree count/ fixed area plot size

D_{bf} = diameter of tree of average basal area

$= ((BAF \times k)/0.005454\,n)^{1/2}$

Now substituting

$N = n$

$\Sigma D = nD_{bf}$

$\Sigma D^2 = (BAF \times k)/0.005454$

into Gingrich's equation we have

$SSP = (-0.0507n + 0.1698nD_{bf} + (0.0317BAF\,k)/0.005454)/10$

or

$SSP = -0.00507n + 0.2299\,n\,((BAF \times k)/n)^{1/2} + 0.58122\,BAF \times k.$

The second method uses only the trees sampled from a variable area plot. In this case sample tree diameters must be measured.
Thus

$n = \sum_{i=1}^{k} BAF/0.005454d_i^2 \quad i = 1, 2, \ldots, k;$ k sample trees

$= (BAF/0.005454) \sum_{i=1}^{k} 1/d_i^2$

$\Sigma D = \sum_{i=1}^{k} (BAF/0.005454d_i^2)\,d_i$

$= (BAF/0.005454) \sum_{i=1}^{k} 1/d_i$

$\Sigma D^2 = \Sigma(BAF/0.005454d_i^2)\,d_i^2$

$= (BAF \times k)/0.005454$

[1] *Gingrich, S. F. 1967. Measuring and evaluating stocking and stand density in upland hardwood forests in the Central States. For. Sci. 13:38-53.*

and substituting

$$SSP = (-0.0507 \frac{BAF}{0.005454} \sum_{i=1}^{k} \frac{1}{d_i^2}$$

$$+ 0.1698 \frac{BAF}{0.005454} \sum_{i=1}^{k} \frac{1}{d_i}$$

$$+ 0.0317 \frac{BAF * k}{0.005454})/10$$

or

$$SSP = \frac{BAF}{10} (5.8122k + 31.1331 \sum_{i=1}^{k} \frac{1}{d_i}$$

$$-9.2959 \sum_{i=1}^{k} \frac{1}{d_i^2})$$

Note that when BAF = 10 then

$$SSP = 5.8122k + 31.1331 \sum_{i=1}^{k} \frac{1}{d_i} -9.2959 \sum_{i=1}^{k} \frac{1}{d_i^2}.$$

Frequently, in addition to stocking we need to know the diameter of the tree of average basal area. For the variable plus fixed plot method this is

$$D_{bf} = \left(\frac{k * BAF}{0.05454n} \right)^{1/2}$$

and for the variable plot method is

$$D_{bv} = \left(\frac{k}{\frac{1}{d^2}} \right)^{1/2}$$

The stocking and average diameter equations differ in each method by the way in which the number of trees per acre are obtained. These differences affect the estimate obtained by each method. From these equations we can see that the variability of point sample estimates increase as the variability of tree diameters increase among points whereas among plots the variability of estimates are related to the variability in the number of trees sampled among plots.

Thus the variability of stocking and average diameter estimates is sensitive to the distribution of tree diameters within a stand. To see how each method compares in its ability to estimate stocking and average diameter in stands with different diameter distributions, I simulated the sampling process on a computer using four stands that had different diameter distributions (fig. 1). Trees were located randomly within each stand. Then for each stand 10 points were selected and 1/20 acre circular plots were located with their center at each point. For each sampling method stand stocking percent and mean stand diameter were averaged over the 10 points. This procedure was repeated 100 times while keeping tree location constant. In addition, stocking and average diameter were calculated using all trees in the stand and these were designated as true values.

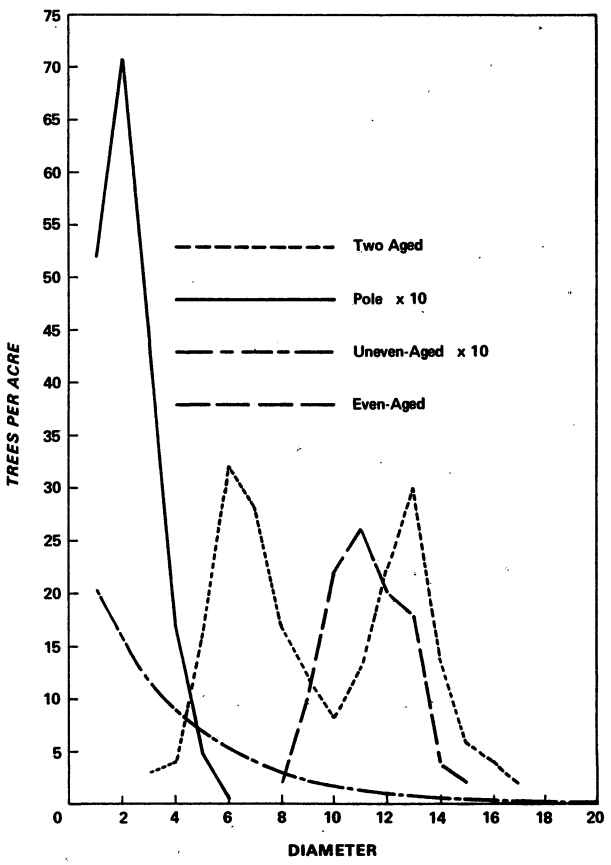

Figure 1. — *Diameter structures of two aged, pole, uneven-aged, and even-aged stands.*

Each method estimated stocking percent with about the same accuracy except the uneven-aged stand was estimated more closely by the variable plus fixed plot method (fig. 2). The variable plot method deviated farthest (underestimated) true stocking percent and had a variance 1⅓ times greater than that of the variable plus fixed plot method for the uneven-aged stand.

The comparison of average diameter revealed that the methods were similar in their estimates for the two-aged and pole-sized stands (fig. 3). But, their estimates were not similar for the even- and uneven-aged stands. In uneven-aged stands estimates obtained from the point sample are biased upward and the variance is 3½ times larger than for the point plus fixed plot method. In the even-aged stand the pattern in variance is reversed, but estimates are not biased.

Therefore, point sampling methods alone should not be used to estimate stocking and average diameter in uneven-aged stands. But the point sampling method can be used to provide estimates of stocking and average stand diameter in stands having distributions similar to the other three studied with a reliability equal to or better than the combination method. In particular, for stands having diameter distributions like the even-aged stand presented here, estimates of mean stand diameter obtained by point sampling tend to be more reliable than those obtained by using the combination method.

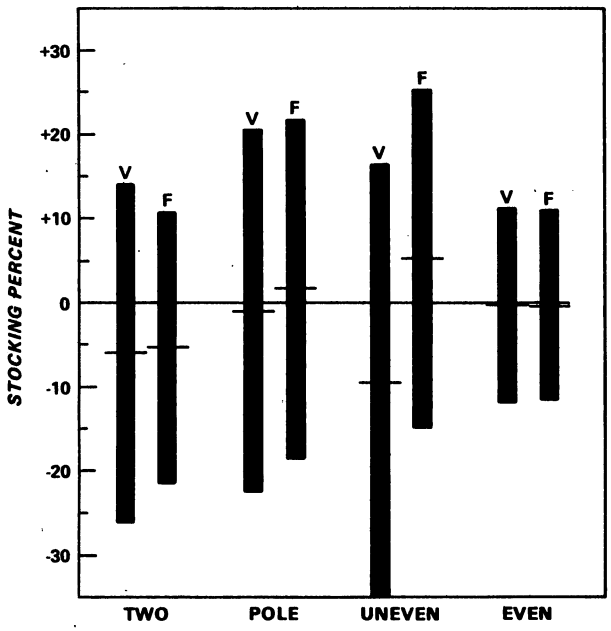

Figure 2. — *A comparison of stocking precent estimates based on 100 averages of 10 points in four stands using variable area plot (V) and variable area plot plus fixed area plot (F) sampling methods. Lines through bars represent estimates of true value of stocking percent (line at 0) and vertical scale shows deviation values.*

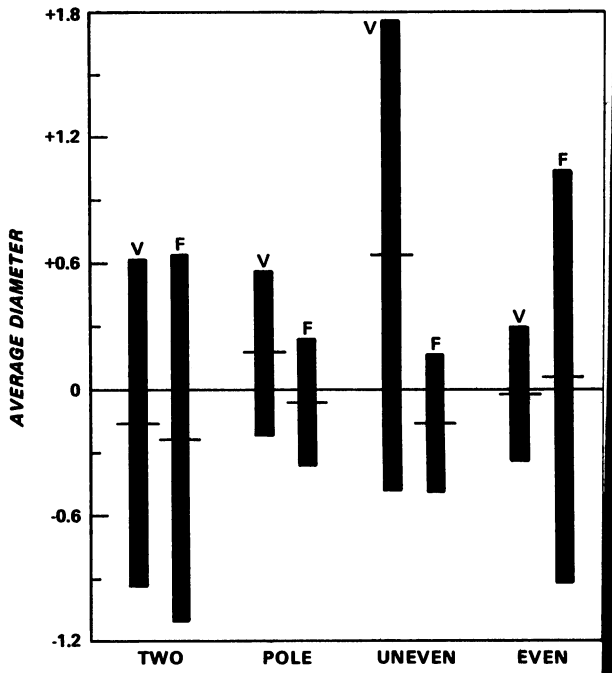

Figure 3. — *A comparison of mean stand diameter (tree of average basal area) estimates based on 100 averages of 10 points in four stands using variable area plot (V) and variable area plot plus fixed area plot (F) sampling methods. Lines through bars represent estimates of true value of mean stand diameter (line at 0) and vertical scale shows deviation values.*

NONLINEAR BASAL AREA GROWTH MODELS FOR RED PINE

Chung-Muh Chen, *Forest Biometrician, Minnesota Department of Natural Resources, St. Paul, Minnesota*

and **Dietmar W. Rose,** *Associate Professor, University of Minnesota, St. Paul, Minnesota*

Previous models of individual tree growth have been based on the open-grown tree concept (Newnham 1964, Arney 1974, Ek and Monserud 1974) and on empirical functions (Bella 1971, Tennent 1975, Moore *et al.* 1973, Adlard 1974). In the open-grown tree approach, individual tree size is assumed to be maximum if the tree is grown in the open (free from competition); the maximum size is reduced if the tree is grown in a stand (subject to competition).

Most periodic growth models for individual trees express the amount of competition a tree receives from its neighbors. Many view competition between trees in terms of zones of influence (Staebler 1951, Newnham 1964, 1966, Opie 1968, Bella 1971, Gerrard 1969, Arney 1974, Keister 1971, Ek and Monserud 1974). The basic assumption is that competition between individual trees occurs only when their zones overlap.

The objectives of this study were to formulate nonlinear biological basal area growth models and to analyze the relation between individual tree competition and growth. We used data from an even-aged red pine plantation near Star Lake, Wisconsin.[1] Initial spacing of the plantation was 6 by 6 feet. Site index was 65 at age 50 and tree survival was high on the site (Wilson 1963).

[1] *The data were provided by Dr. Alan R. Ek, University of Minnesota, College of Forestry, and Wisconsin Department of Natural Resources.*

FORMULATION OF NONLINEAR BASAL AREA GROWTH MODEL

Periodic basal area growth can be related to potential basal area increment when the immature tree is free from competition. This growth can then be reduced by a competition factor when the tree is grown under competition. This relation can be shown by the following equations:

$$\Delta B = \Delta B^* [1 - e^{-k(1/c)m}]^N \quad (1)$$

$$\text{or } \Delta B = \Delta B^* e^{-kC} \quad (2)$$

where ΔB = the periodic tree basal area growth of the tree,

ΔB^* = the potential growth when the tree is free from competition,

C = the competition index of the tree,

k, m, and N = growth factors such as site, species, age, and density.

As $C \uparrow$, $\Delta B \downarrow$; as $C \downarrow$; $\Delta B \uparrow$

$\lim_{C \to 0} \Delta B = \Delta B^*$ for $k > 0, m > 0$

$\lim_{C \to \infty} B = 0$ for intolerant species.

The advantage of the models (equations 1 and 2) is that they offer a logical explanation of the relation between the dependent and independent variables. However, the potential growth of a tree might not be realized not only because of

competition, but also because of disease, insects, animals, wind, frost, etc. Furthermore, the model is less useful for predicting growth of intermediate and suppressed trees when they are completely released because these trees may not regain their full potential growth. So the condition that

$\Delta B \rightarrow \Delta B^*$ as $C \rightarrow 0$

may not be fully realized.

An alternative approach is to assume that tree periodic basal area growth is directly related to site, initial basal area, and functional crown surface, and inversely related to competition index. Functional crown surface is correlated with tree growth. Tree height or basal area are correlated with the functional crown surface for immature individual trees growing in dense even-aged stands (not stagnant) of single intolerant species. Therefore, in the case of lacking information on tree height and functional crown surface, initial tree basal area or diameter breast height and competition index may predict tree periodic basal area increment. For this study, we define two models similar to equations 1 and 2, except ΔB^* was replaced by "a B^b"; where B is the basal area of the tree at the beginning of the growth period and a and b are two additional factors.

MEASURE OF TREE COMPETITION

The competition imposed on a tree is measured by the distance to the competing tree, amount of overlap area, and relative size. It is formulated in the following manner:

$$C_i = (1/A_i) \sum_{j=1}^{N} 0_{ij} W_{ij} \qquad (3)$$

where C_i = the competition index of tree i,

A_i = the area of the influence zone or circle about the sample tree i with the radius (P_i) proportional to the tree diameter,

P_i = 1, 1.5, 2.0, 2.5,

O_{ij} = the area of overlap between tree i and its competitor j for j = 1, 2, . . ., N_i,

N_i = number of competitors of tree i,

W_{ij} = a weighting factor for O_{ij}.

We used the following weighting factor:

$$W_{ij} = R\,[\,1 - \exp(-k_1 r_{ij})]^n \qquad (4)$$

where

$r_{ij} = (d_j/d_i)^E$ and d_j/d_i is the ratio of diameters of tree i and its competitor j,

$R = \max (d_j/d_i)^E$ for all trees (i, j) with overlapping influence zones,

k_1 and E are factors related to species, age, site, and density (E = 1 to 4).

$$k_1 = -\log\,[\,1-(1/R)^{\frac{1}{n}}] \qquad (5)$$

when weighting factor $W_{ij} = 1$ is assigned for the condition $d_i = d_j$, n was assigned the value 1 or 2.

As $r_{ij} \rightarrow 0$, $W_{ij} \rightarrow 0$;
$r_{ij} \rightarrow \infty$, $W_{ij} \rightarrow R$;

and as
$r_{ij} \rightarrow 1$, $W_{ij} \rightarrow 1$.

The weighting factor for modifying the overlap area between a tree and its competitor should reflect the potential size difference of the sample tree i and its competitor j.

RESULTS AND DISCUSSION

Approximately optimal values of Pi and E (for equations 3 and 4) for standard error and correlation of regression between basal area growth and competition index were derived via iteration (table 1). Bella's (1971) index generated comparable results. When no iterations on E and n were performed, i.e., E = n = 1 Chen's (1976) model resulted in correlations that were approximately 10 percent higher. A modification of Gerrard's (1969) index (inclusion of the exponent E) proved somewhat inferior to the two other indexes, but is easier to calculate. The indexes will have to be compared using different species, ages, and stand conditions.

For predicting individual tree growth one of the two proposed basal area growth models was fitted via nonlinear regression (table 2). The

Table 1. — *Correlation between periodic basal area growth and competition index for three competition models*[1]

Plot[2]	Observations		Coefficient of Determination[5]		Standard error	Standard Regression Coefficients		
	Total[3]	Regression[4]	Adjusted	Unadjusted		a	b	k
					Inch[2]			
1	186	17	0.55	0.85	2.84	34.63	-0.4571	1.5557
2	203	20	.52	.86	2.16	3.25	.1137	0.7839
3	269	19	.88	.95	0.52	0.043	1.2744	.2038
1, 2, & 3 combined	658	56	.60	.86	1.81	1.38	.3682	.7912
4	296	24	.56	.80	5.17	3134.23	-1.4585	1.9977

[1]$\Delta B = aB^b (\exp(-kC))$
ΔB = the periodic tree basal area growth in square inches.
C = the competition index (equation 3) with weighting factor (equation 4).
Parameter E = 2, R = 1, n = 2 used for all in calculation of competition index.
[2]Stand age 32-37.
[3]Total observations used for calculating competition index.
[4]Number of trees for which growth and competition was determined.
[5]The coefficient of determination adjusted for the mean measures the contribution of the sample mean in explaining variance of the dependent variable.

Table 2. — *Nonlinear regression gits for a nonlinear basal area growth models*[1]

Plot[2]	r	Standard error	E[3]	Pi[4]	n	Remarks
Inch[2]		*Inch*[2]				
1	-0.82	1.26	2	1	2	Chen (1976) model
2	-0.72	1.41	2	2.5	1	$W_{ij} = (1-e^{-k_1(d_j/d_i)^E})^n$
3	-0.73	1.60	2	1.0	2	(equation 4)
4	-0.70	2.42	1.5	1.0	2	
1	-0.82	1.27	3.5	1.0	-	Bella (1971)
2	-0.72	1.42	2.0	2.5	-	
3	-0.73	1.60	4.0	1.0	-	$W_{ij} = (d_j/d_i)^E$
4	-0.70	2.43	1.5	1.0	-	
1	-0.72	1.50	4	2.5	-	modified Gerrard index
2	-0.63	1.57	4	2.0	-	
3	-0.72	1.62	4	1.0	-	$C_i = \Sigma \left(\frac{O_{ij}}{A_i}\right)^E$ and
4	-0.63	2.63	2	1.0	-	$W_{ij} = 1$

[1]$\Delta B_i = ae^{-kC_i}$ or $\log \Delta B_i = \log a - kC_i$ where $C_i = \sum_{j=1}^{N_i} \frac{O_{ij}}{A_i} W_{ij}$ (competition index) and W_{ij} is a weighting factor.

[2]Plot age 32-37;plots 1 to 3 are control plots and plot 4 is a thinned plot.

[3]E = parameter of competition index

[4]Pi = proportionality factor for radius of zone of influence of subject tree and tree diameter.

model adequately explained basal area growth as a function of basal area and competition for the first three plots. The large standard error for the thinned plot (plot 4) indicates a much poorer fit.

Further work is underway to test those models using more plots and different species and ages. Preliminary results indicate less satisfactory fits for an older plot of the Star Lake plantation (age 58-65). Relative diameters or basal areas are adequate weighting factors only in some instances. It will be necessary to find weighting factors that better reflect the potential size increment of the sample tree i and its competitor j such as height, crown ratio, live crown length, or functional crown surface or volume. These variables may improve the growth models for red pine as well as for other species in even-aged stands. Species tolerance will have to be considered if the competition model is applied to mixed stands (Chen 1976).

LITERATURE CITED

Adlard, P.G. 1974. Development of an empirical competition model for individual trees within a stand. In *Growth models for tree and stand simulation. Int. Union of For. Res. Org. Working Party S4.01-4, Proc., 1973. J. Fries, ed., Royal Coll. For., Stockholm, Sweden. p. 22-37.*

Arney, J. D. 1974. Stand simulators — The forester's tool. In *Use of competers in forestry. P. J. Fogg and T. D. Keister., eds. Div. Cont. Education, Louisiana State Univ., Baton Rouge, Louisiana. p. 59-72.*

Beck, D. E. 1974. Predicting growth of individual trees in thinned stands of yellow poplar. In *Growth models for tree and stand simulation. Int. Union of For. Res. Org. Working Party S4.01-4, Proc., 1973. J. Fries, ed., Royal Coll. For., Stockholm, Sweden. p. 47-55.*

Bella, D. E. 1970. Simulation of growth, yield and management of aspen. Ph.D. thesis, Univ. British Columbia, Canada. 190 p.

Bella, D. E. 1971. A new competition model for individual trees. For. Sci. 17:364-372.

Chen, Chung-Muh. 1976. Dynamics of an even-aged stand — structure, mortality, competition and growth. Ph.D. thesis, Univ. Minnesota, Coll. For., St. Paul, Minnesota. 107 p.

Ek, Alan R., and Robert A. Monserud, 1974. Forest: A computer model for simulating the growth and reproduction of mixed species forest stands. Res. Rep. R2635, 13p. Dep. For., Univ. Wisconsin, Madison, Wisconsin.

Gerrard, Douglas J. 1969. Competition quotient: A new reasure of the competition affecting individual forest trees. Agric. Exp. Stn. and Michigan State Univ. Res. Bull. 20, 32 p.

Hatch, R. C., Douglas J. Gerrard, and J. C. Tappeiner. 1975. Exposed crown surface area: a mathematical index of individual tree growth potential. Can. For. Res. 5:224-228.

Keister, T. D. 1971. A measure of the intraspecific competition experienced by an individual tree in a planted stand. Louisiana State Univ. Agric. Exp. Stn. Bull. 652, 30 p.

Moore, J. A., C. A. Budelsky, and Richard C. Schlesinger. 1973. A new index representing individual tree competitive status. Can. J. For. Res. 3:495-500.

Newnham, R. M. 1964. The development of a stand model for Douglas-fir. Ph. D. thesis, Univ. British Columbia, Vancouver. 201 p.

Newnham, R. M. 1966. Stand structure and diameter growth of individual trees in a young red pine stand. Can. Dep. For., For. Manage. Res. and Serv. Inst., Unpubl. Intern. Rep. FMR-1, 19 p.

Opie, J. E. 1968. Predictability of individual tree growth using various definitions of competing basal area. For. Sci. 14(3):314-323.

Staebler, G. R. 1951. Growth and spacing in an even-aged stand of Douglas-fir. Unpubl. M. F. thesis, Univ. Michigan. 54 p.

Tennent, R. B. 1975. Competition quotient in radiata pine. For. Res. Inst. Private Bag. Rotorua, New Zealand. 7 p.

Wilson, F. G. 1963. Fifty years from seed — The Star Lake plantation. Wisconsin Conserv. Dep. Tech. Bull. 27, 24 p.

DISCRETE TIME MARKOV PROCESSES

John W. Moser, Jr., *Professor of Forestry, Purdue University, West Lafayette, Indiana*

By observing the evolution of natural phenomena, it is readily apparent that events occur that are not entirely predictable. The modeling of such events is often facilitated by employing random processes. The intent of this paper is to consider and to illustrate a subclass of the set of stochastic processes — one known as discrete time Markov models. This subclass is termed discrete time because time is indexed in finite steps rather than as a continuum. Diameter class distributions in forest stands will be used to illustrate the process.

A Markov chain is a discrete time stochastic process consisting of a sequence of random events $\{ X_1, X_2, X_3, \ldots \}$, each with a finite number of possible outcomes $\{ a_1, a_2, \ldots, a_r \}$ (Phillips *et al.* 1976) This set of possible outcomes is termed state space. The value assumed by X_i is called the state of the process at time i. It is assumed that the random variable, X_i, depends only upon the previous event X_{i-1}, and affects only the subsequent one, X_{i+1}. This assumption, known as the Markov assumption, avoids having to express joint distributions for all events at one time. Instead, it is sufficient to express conditional distributions of just two neighboring random variables at a time. Markov's assumption simplifies the problem but does not completely eliminate the dependence between random variables. Therefore life processes can be realistically represented.

Given that $X_0 = a_i$ is the present state of a process, one desires to know the probability distribution of the possible outcomes for X_1. These transitional probabilities are designated p_{ij}, which represent the conditional probability of going from state a_i to state a_j after one step or transition, i.e., $P\{ X_1 = a_j | X_0 = a_i \}$.

A conventional means of exhibiting transition probabilities is with a square matrix. A transition matrix for a three-state process may be represented as:

$$P = (p_{ij}) = \begin{array}{c} \\ a_1 \\ a_2 \\ a_3 \end{array} \begin{array}{c} \begin{array}{ccc} a_1 & a_2 & a_3 \end{array} \\ \begin{bmatrix} p_{1,1} & p_{1,2} & p_{1,3} \\ p_{2,1} & p_{2,2} & p_{2,3} \\ p_{3,1} & p_{3,2} & p_{3,3} \end{bmatrix} \end{array}$$

Because each row of the above matrix represents a probability distribution for X_1, $\sum_j p_{ij} = 1$ for each i.

The matrix P completely describes the process for any given outcome at X_1 given its initial dependence upon X_0. If event X_1 is described, the probability distribution for X_2 must be developed. By the Markov assumption, the next state, X_2 in this instance, depends only upon the previous state, X_1. However, X_1 depends upon X_0. Three mutually exclusive paths exist to progress from $X_0 = a_1$ to $X_2 = a_1$ (fig. 1). The probability of being in state a_1 at time 2 given that the process was in state a_1 at time o may be represented as the sum of the three "path probabilities":

$$\begin{aligned} P\{ X_0 = a_1 \rightarrow X_2 = a_1 \} = & \\ & P\{ X_0 = a_1 \rightarrow X_1 = a_1 \rightarrow X_2 = a_1 \} \\ & + P\{ X_0 = a_1 \rightarrow X_1 = a_2 \rightarrow X_2 = a_1 \} \\ & + P\{ X_0 = a_1 \rightarrow X_1 = a_3 \rightarrow X_3 = a_1 \} \quad (1) \end{aligned}$$

By employing the Markov assumption and the matrix of one-step transition probabilities, Equation (1) can be rewritten as:

$$\begin{aligned} P\{ X_0 = a_1 \rightarrow X_2 = a_1 \} = & \\ & p_{1,1} \; P\{ X_1 = a_1 \rightarrow X_2 = a_1 \} \\ & + p_{1,2} \; P\{ X_1 = a_2 \rightarrow X_2 = a_1 \} \\ & + p_{1,3} \; P\{ X_1 = a_3 \rightarrow X_2 = a_1 \}. \end{aligned}$$

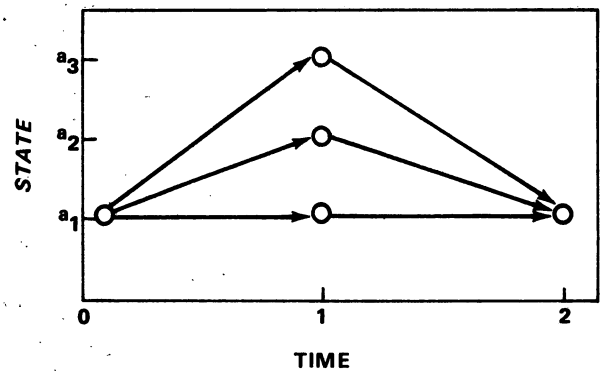

Figure 1. — Possible transitions from $X_0 = a_1$ to $X_2 = a_1$ for a three-state process.

The probability for the first leg of each path is readily obtained from the matrix of one-step probabilities. The probabilities for the second step of each path is really the transition probability associated with the second transition. At this point an additional simplifying assumption is needed. If it is assumed that the transitional probabilities do not change with time, then:

$$P\{X_0 = a_1 \rightarrow X_2 = a_1\} = p_{1,1}\,p_{1,1} + p_{1,2}\,p_{2,1} + p_{1,3}\,p_{3,1}. \quad (2)$$

The assumption is known as stationarity; without it the process would not be able to continue because a new transition matrix would be needed for each transition. Using similar logic, probabilities may be developed for other states at X_2 given that $X_0 = a_1$:

$$P\{X_0 = a_1 \rightarrow X_2 = a_2\} = p_{1,1}\,p_{1,2} + p_{1,2}\,p_{2,2} + p_{1,3}\,p_{3,2}. \quad (3)$$

$$P\{X_0 = a_1 \rightarrow X_2 = a_3\} = p_{1,1}\,p_{1,3} + p_{1,2}\,p_{2,3} + p_{1,3}\,p_{3,3}. \quad (4)$$

Thus, Equations (2), (3), and (4) specify the probability distribution of X_2, given that $X_0 = a_1$. Similarly, other expressions may be developed to specify the probability distribution for X_2 given that $X_0 = a_2$ or $X_0 = a_3$. The notation $p_{ij}^{(2)}$ is utilized for the individual elements of the two-step transition matrix and the complete two-step matrix, $P^{(2)}$, for the three-state process may be represented as:

$$P(2) = p_{ij}^{(2)})) \quad \begin{bmatrix} p_{1,1}^{(2)} & p_{1,2}^{(2)} & p_{1,3}^{(2)} \\ p_{2,1}^{(2)} & p_{2,2}^{(2)} & p_{2,3}^{(2)} \\ p_{3,1}^{(2)} & p_{3,2}^{(2)} & p_{3,3}^{(2)} \end{bmatrix}$$

As indicated above, the individual elements are calculated from the one-step matrix:

$$p_{1,1}^{(2)} = p_{1,1}\,p_{1,1} + p_{1,2}\,p_{2,1} + p_{1,3}\,p_{3,1}.$$

The two-step transition matrix is obtained by squaring the one-step matrix:

$$P^{(2)} = P \,.\, P = P^2 \quad (5)$$

The relation expressed in Equation (5) is only possible by use of the Markov and stationarity assumptions.

To obtain the distributions of X_3 given various possible states of X_0, it is again necessary to consider possible paths that lead from X_0 to X_3 in a similar fashion as was illustrated for X_2. Following that logic, the elements of the three-step transition matrix can be written in terms of the two-step and one-step probabilities:

$$p_{1,1}^{(3)} = p_{1,1}^{(2)}\,p_{1,1} + p_{1,2}^{(2)}\,p_{2,1} + p_{1,3}^{(2)}\,p_{3,1}.$$

In matrix notation that is:

$$P^{(3)} = p^{(2)} \,.\, p = p^2 \,.\, p = p^3.$$

The n-step transition matrix is equal to the one-step transition matrix raised to the nth power,

$$P^{(n)} = P^n. \quad (6)$$

The relation expressed by Equation (6) is the most important result for Markov chains because it gives the probability of being in a particular state at a particular time, given the initial state.

To illustrate the use of the discrete time Markov model, data were obtained from permanent growth plots in a central Wisconsin mixed hardwood stand that had been measured for diameter for 19 consecutive years. The 25 states chosen for the model are the 1-inch diameter classes from 8-inch through 29-inch, a diameter class called > 29 inch, and the categories of death and harvest. The 8-inch class was the lowest diameter class in which all trees were measured and

31-inch was the largest diameter of any tree after 19 years. Because only the first nine growth periods were utilized to develop the model, it was necessary to define the largest diameter class as > 29 to obtain numerical values for the transition probabilities.

A tree in any state representing a diameter class may either remain in that class, move to a higher class, die, or be harvested. The dead and harvest states are considered absorbing states because once a tree has entered either one of these states it cannot leave it. The 1-inch diameter classes are termed transient states.

The information to determine the probabilities for transitions between states and to verify the predictive ability of the model was obtained by summarizing the progression of the initial trees in each diameter class for the 19-year period (table 1). Ingrowth trees were not included in the summaries.

If a tree was in the 10-inch diameter class 9 years ago, the transition probabilities associated with its movement are determined as follows: (1) the tree will remain in the 10-inch class, $p_{1,0,1,0}$, = 44/139; (2) the tree will advance to the 11-inch class, $p_{1,0,1,1}$, = 81/139; (3) the tree will move into the 12-inch class, $p_{1,0,1,2}$, = 5/139; (4) the tree will die, $p_{1,0,m}$ = 8/139; or (5) the tree will be harvested, $p_{1,0,c}$ = 1/139.

The transition probabilities for the other diameter classes are similarly determined with the respective diameter class progression summaries. Because death and harvest are absorbing states, $p_{m,m} = p_{c,c} = 1$ (table 2).

As indicated by Equation (5), the two-step transition probabilities are obtained by squaring the initial transition matrix. The numbers $p_{ij}^{(2)}$ for i and j = 8 . . . 29, > 29, M[1], and C given the probability of a tree being in state j given that it was in state i two steps ago (table 3).

If $t^{(0)} = (t_8^{(0)}, t_9^{(0)}, \ldots, t_{29}^{(0)}, t_{>29}^{(0)}, t_m^{(0)}, t_c^{(0)})$ is a vector whose elements correspond to the initial number of trees in each state, then the matrix of two-step transition probabilities can be used to predict the disposition of those initial trees after 18 growing seasons. The numbers $p_{im}^{(2)}$ and $p_{ic}^{(2)}$ for i = 8 . . . 29, >29 are, respectively, the death and harvest probabilities for a tree given that it was initially in the ith diameter class. The predicted number of mortality trees, m_i, and harvested trees, c_i, are:

$$m_i = t_i^{(0)} \cdot p_{im}^{(2)} \quad (7)$$

and

$$c_i = t_i^{(0)} \cdot p_{ic}^{(2)} \text{ for } i = 8 \ldots 29, > 29. \quad (8)$$

Because Equations (7) and (8) account for death and harvest, the number of surviving trees, s_i, from each initial diameter class is

$$s_i = t_i^{(0)} \cdot (1 - p_{im}^{(2)} - p_{ic}^{(2)}) \quad (9)$$
$$\text{for } i = 8 \ldots 29, > 29.$$

Equation (9) indicates the number of trees in the ith diameter class expected to survive. It does not indicate the distribution of the surviving trees.

To determine the diameter distribution for surviving trees it is necessary to sum all the ways that a tree can enter a diameter class, regardless of its initial class:

$$t_j^{(2)} = \sum_i t_i^{(0)} \cdot p_{ij}^{(2)} \quad (10)$$

[1] *M = dead trees; C = harvested trees.*

Table 1. — *The progression of all trees initially in the 10-inch diameter class by number of trees and change in diameter class*
(In number of trees)

Diameter class (in.)	Measurement 1	2	3	4	5	6	7	8	9	10	11	12	13	14	15	16	17	18	19
10	139	133	115	107	98	83	69	62	61	44	41	35	29	25	22	19	16	15	13
11	0	5	23	31	37	50	61	68	68	81	75	75	69	67	66	67	67	60	56
12	0	0	0	0	0	0	2	2	2	5	12	18	29	34	35	36	37	38	38
13	0	0	0	0	0	0	0	0	0	0	2	2	2	2	3	4	6	10	12
14	0	0	0	0	0	0	0	0	0	0	0	0	0	1	2	2	2	2	2
15	0	0	0	0	0	0	0	0	0	0	0	0	0	0	0	0	0	0	1
Total	139	138	138	138	135	133	132	132	131	130	130	130	129	129	128	128	128	125	122
Total mortality		1	1	1	4	6	7	7	7	8	8	8	9	9	10	10	10	13	15
Total cut		0	0	0	0	0	0	0	1	1	1	1	1	1	1	1	1	1	2

Table 2. — *The initial matrix of transition probabilities based on ratios from measurements 1 and 10*

Diameter class: at measurement:[1] (inches)	Diameter class at measurement 10 (inches): 8	9	10	11	12	13	14	15	16	17	18	19	20	21	22	23	24	25	26	27	28	29	>29	M[1]	C[1]
8	0.37	0.48	0.04																					0.09	0.01
9		.39	.44	0.04	0.01																			.11	.02
10			.32	.58	.04																			.06	.01
11				.27	.50	0.17	0.01																	.04	.02
12					.24	.55	.12																	.04	.04
13						.17	.50	0.21																.11	.02
14							.20	.53	0.19															.05	.02
15								.12	.59	0.22	0.01													.02	.03
16									.12	.54	.18													.09	.07
17										.11	.56	0.23												.06	.03
18											.08	.52	0.23	0.04										.08	.06
19												.03	.50	.16	0.03									.09	.19
20													.04	.54	.27									.00	.15
21														.07	.57	0.29								.00	.07
22															.12	.12	0.38	0.12						.00	.25
23																	.67	.22						.00	.11
24																	.17	.33	0.33					.00	.17
25																			.67	0.33				.00	.00
26																				.50	0.00	0.17		.17	.17
27																					.00	.40	0.00	.40	.20
28																						.50	0.50	.00	.00
29																						.25	.50	.25	.00
>29																								1.0	.00
M[1]																								1.0	.00
C[1]																									1.0

[1]M = dead trees; C = harvested trees.

Table 3. — *Two-step transition probabilities (found by squaring the matrix of table 2)*

Diameter class: at measurement:[1] (inches)	Diameter class at measurement 19 (inches): 8	9	10	11	12	13	14	15	16	17	18	19	20	21	22	23	24	25	26	27	28	29	>29	M[1]	C[1]
8	0.14	0.36	0.24	0.05	0.01																			0.18	0.03
9		.15	.31	.28	.04	0.01																		.18	.03
10			.10	.34	.31	.12	0.01																	.10	.02
11				.07	.26	.35	.15	0.04																.09	.05
12					.06	.23	.32	.18	0.02															.12	.07
13						.03	.18	.32	.22	0.05														.16	.04
14							.04	.17	.38	.22	0.04													.09	.06
15								.01	.14	.37	.23	0.06												.10	.09
16									.01	.12	.34	.22	0.04											.15	.10
17										.01	.10	.32	.25	0.06	0.01									.13	.11
18											.01	.06	.29	.21	.10	0.01								.13	.20
19													.03	.29	.23	.05	0.01							.10	.29
20														.06	.35	.19	.10	0.03						.00	.27
21														.01	.11	.09	.40	.13						.00	.25
22															.02	.02	.19	.17	0.21	0.04				.00	.36
23																	.11	.22	.37	.07				.00	.22
24																	.03	.06	.28	.28	0.00	0.06		.06	.25
25																				.33	.00	.24		.24	.18
26																					.00	.24	0.08	.41	.27
27																					.00	.10	.20	.50	.20
28																						.12	.25	.62	.00
29																						.06	.12	.81	.00
>29																								1.0	.00
M[1]																								1.0	.00
C[1]																									1.0

[1]M = dead trees; C = harvested trees.

where $t_j^{(2)}$ is the number of trees in state j after two transitions, regardless of the initial state.

If the values obtained from Equation (10) are defined in vector form as
$t^{(2)} = (t_8^{(2)}, t_9^{(2)}, \ldots, t_{29}^{(2)}, t > 29^{(2)}, t_m^{(2)}, t_c^{(2)})$, then the equation

$$t^{(2)} = t^{(0)} \cdot p^{(2)}$$

may be used to obtain the individual elements.

The elements $t_m^{(2)}$ and $t_c^{(2)}$ of $t^{(2)}$ are equivalent to the $\Sigma_i m_i$ and $\Sigma_i c_i$ from Equations (7) and (8), respectively. The total number of surviving trees equals

$$\sum_i s_i = \sum_i t_i^{(2)} \text{ for } i = 8 \ldots 29, > 29.$$

Thus, this value may be determined as the sum of the elements from Equation (9) or from the sum of all elements of the vector $t^{(2)}$ except death and harvest.

The foregoing relations may be utilized to predict diameter distributions. We demonstrated the predictive ability of the model by using data collected from a stand for 19 consecutive years (table 4). The observed and predicted values agree closely; however, the number of surviving trees by initial diameter class is more accurately predicted than the distribution of surviving trees (Bruner and Moser 1973).

In another study (Cassell and Moser 1974) the trees were grouped into six tolerance classes and each class was individually modeled to provide information on species composition and diameter distribution (tables 5 and 6). The results from this study are similar to those of the composite model. In general the predicted number of surviving trees by species group was accurate and the prediction of death, harvest, and future diameter distribution somewhat less accurate.

For both of the above studies, the basic data were utilized to develop additional models with transition periods of 4, 5, 6, 7, and 8 years. Predictions obtained with these models were similar to those of the 9-year model. Further, it was indicated that the accuracy of prediction was not dependent upon the length of the prediction period but that predictions beyond one period were less accurate.

To utilize the Markov process, the Markov and stationarity properties must be satisfied. First, to predict the next state the present state must be known. Second, the transition probabilities between two specific states must remain constant. In regard to the dynamics of diameter distributions, these properties imply that: (1) the diameter distribution some time in the future

Table 4. — *Observed and predicted stand values at measurement 19 using composite model*
(In number of trees)

d.b.h. class (inches)	Initial no. trees	Survivors Actual	Survivors Predicted	Diameter Distribution Actual	Diameter Distribution Predicted	Mortality Actual	Mortality Predicted	Harvested Actual	Harvested Predicted
8	209	175	165	22	28	29	37	5	6
9	148	117	117	97	98	23	26	8	5
10	139	122	122	116	109	15	14	2	3
11	131	110	113	116	108	14	12	7	6
12	111	91	90	94	91	10	14	10	8
13	107	85	86	72	92	14	17	8	4
14	88	76	75	85	79	7	8	5	5
15	86	73	70	74	75	4	8	9	7
16	74	54	55	75	73	8	11	12	8
17	64	50	48	67	66	8	9	6	7
18	52	35	35	67	56	6	7	11	10
19	32	19	20	51	45	3	3	10	9
20	26	19	19	24	35	1	0	6	7
21	14	11	11	36	26	1	0	2	3
22	8	5	5	16	24	0	0	3	3
23	9	5	7	18	8	0	0	4	2
24	6	3	4	7	11	1	0	2	2
25	3	3	2	8	7	0	1	0	1
26	6	3	2	2	7	1	2	2	2
27	5	2	2	7	4	2	3	1	1
28	4	1	2	2	0	2	3	1	0
29	4	3	1	0	4	1	3	0	0
> 29	1	0	0	6	3	1	1	0	0
Totals	1,327	1,062	1,051	1,062	1,049	151	179	114	98

Table 5. — *Observed and predicted survivor distributions at measurement 19 using tolerance class model*
(In number of trees)

d.b.h. class (inches)	Composite distributions			Final distributions											
				Class 1		Class 2		Class 3		Class 4		Class 5		Class 6	
	Initial	Final	Predicted	Actual	Predicted	Actual	Predicted	Actual	Predicted	Actual	Predicted	Actual	Predicted	Actual	Predicted
8	209	22	29	1	1	1	4	18	23	1	1	0	0	1	1
9	148	97	99	5	7	13	12	75	76	2	2	0	0	2	2
10	139	116	110	3	6	17	18	85	83	7	1	0	0	4	2
11	131	116	111	12	9	21	27	76	66	3	4	0	0	4	5
12	111	94	90	7	4	24	22	54	50	8	10	0	0	1	4
13	107	72	92	4	4	15	17	44	63	8	5	0	0	1	1
14	88	85	80	5	4	9	10	61	56	6	9	1	0	3	1
15	86	74	76	3	7	16	13	47	49	5	4	0	0	3	3
16	74	75	71	6	5	11	10	52	50	3	2	0	0	3	3
17	64	67	68	5	2	9	13	46	45	4	3	0	0	3	5
18	52	67	56	3	5	12	7	41	39	6	3	0	0	5	1
19	32	51	46	5	4	5	7	36	30	4	2	0	0	1	2
20	26	24	36	1	3	3	5	20	27	0	0	0	0	0	2
21	14	36	24	3	1	4	2	28	20	0	0	0	0	1	1
22	8	16	26	0	0	2	1	14	23	0	0	0	0	0	1
23	9	18	9	0	1	1	2	15	6	0	0	0	0	2	1
24	6	7	11	0	1	1	1	6	9	0	0	0	0	0	0
25	3	8	6	1	0	0	2	7	5	0	0	0	0	0	0
26	6	2	7	0	0	0	1	2	6	0	0	0	0	0	1
27	5	7	4	0	0	0	0	6	4	0	0	0	0	1	1
28	4	2	0	0	0	0	0	2	0	0	0	0	0	0	0
29	4	0	6	0	0	0	0	0	6	0	0	0	0	0	0
> 29	1	6	5	0	0	3	4	2	0	0	0	0	0	1	1
Totals	1,327	1,062	1,062	64	04	167	178	737	736	57	46	1	0	36	38

Table 6. — *Observed and predicted mortality and harvest at measurement 19 using tolerance class model*
(In number of trees)

Class	Measurement 19			
	Mortality		Harvested	
	Actual	Predicted	Actual	Predicted
1	0	1	0	0
2	16	7	13	9
3	31	44	50	38
4	9	19	2	4
5	0	1	0	0
6	1	0	1	1
Totals	57	72	66	52

depends only upon the distribution now and not upon past distributions; and (2) the probability of a tree moving, for instance, from the 8-inch to the 9-inch class in any specific period must remain the same regardless of stand conditions.

The larger discrepancies for predictions beyond one period may be attributable to not satisfying the stationarity assumption. To examine this possibility, the 19 years of remeasurement data were used to determine transition probabilities between the various states over time. These probabilities were fairly constant for diameter classes with a large initial number of trees, but this was not true for diameter classes with a small initial number of trees. This suggests that the accuracy of predictions for several periods is dependent upon good estimates of the transition probabilities which, in turn, are dependent upon sufficient data for all diameter classes. Also, because uneven-aged stands are characterized by a large number of trees in the lower diameter classes, permanent plot data from such stands will have a similar diameter distribution. This situation will inherently lead to greater accuracy in prediction in the lower classes.

Prediction of diameter distributions with the Markov model has both positive and negative points. One disadvantage is that mortality and harvested trees are predicted as numbers of trees by original diameter class so that the actual diameter class of a tree when it dies or is harvested is not known. Another disadvantage is the difficulty of introducing ingrowth into the process. The only way to allow for ingrowth is to inventory trees in diameter classes below the lower limit for which predictions are important. For example, if predictions with ingrowth are desired for sawtimber trees in the 12-inch diameter classes and above, trees in the 8-, 9-, 10-, and 11-inch diameter classes at the initial measurement can be considered as possible ingrowth into the 12-inch and larger classes during the prediction periods. To include ingrowth in all diameter

classes 8 inches and above, trees in roughly the 4-, 5-, 6-, and 7-inch diameter classes would have be inventoried. A third disadvantage is the lack of flexibility in the length of prediction periods. If the two inventory measurements used for the prediction are, for example, 5 years apart, predictions of stand conditions can only be made for subsequent multiples of 5 years. Lastly, at least two measurements from permanent plots are required as data for predictions. This prediction method is not applicable for areas not under a continuous forest inventory system.

Ease of application is a major benefit of the Markov model. Accurate predictions of numbers of survivor, dead, and harvested trees, and the distribution of surviving trees depend only upon conventional continuous forest inventory data and a knowledge of elementary matrix operations.

LITERATURE CITED

Bruner, Harold D., and John W. Moser, Jr. 1973. A Markov chain approach to prediction of diameter distributions in uneven-aged forest stands. Can. J. For. Res. 3(3):409-417.

Cassell, Robert F., and John W. Moser, Jr. 1974. A programmed Markov model for predicting diameter distribution and species composition in uneven-aged forests. Purdue Univ. Agric. Exp. Stn. Res. Bull. 915, 43 p. West Lafayette, Indiana.

Phillips, D. T., A. Ravindran, and J. J. Solberg. 1976. Operations research principles and practices. 585 p. John Wiley and Sons, Inc., New York.

AN ACCURATE WAY TO SELECT SAMPLE PLOTS ON AERIAL PHOTOS USING GROUND CONTROL

Alexander Vasilevsky, *Mensurationist,*
and **Burton L. Essex,** *Principal Resource Analyst,*
North Central Forest Experiment Station,
St. Paul, Minnesota

Most forest inventories begin with the classification of points selected from individual aerial photographs. The information developed from this procedure is subject to several sources of error. Photo cover type classification of a sample point can be in error due to the quality and age of the photos or to the skill of the photo interpreter. These errors can be adjusted by field checking a portion of the photo points. A source of error that cannot be corrected by field checking occurs when end lap (overlap), sidelap, crab, and tilt distort the photo coverage of the land area. This results in some areas being sampled more intensively than others.

The normal forest aerial photography contracts specifies 60 percent endlap and 30 percent sidelap in line of flight. However, the contractor usually delivers more coverage of the area to be sure that these requirements are met. This type of bias is recognized by aerial photo interpreters, but usually ignored in the hope that the errors will be compensating. Contract specifications for aerial photos also require a specific scale — the deviation from specified flight altitudes shall not exceed 300 feet for the purchaser to accept the photos.

We tested photo intensity during the forest survey in Iowa where photographing conditions were good — differences in elevation were moderate and each township had many roads lying north-south and east-west. In spite of these ideal conditions, photo overlap was 0.66 percent greater than specified, which represented 237,000 acres. This means that in sampling individual photos, without regard to overlap variation, area of the predominant land class would have been overestimated. A similar test done by the Pacific Northwest Forest and Range Experiment Station in Oregon and Washington had similar results (Pope *et al.* 1972).

PROCEDURES USED AT OTHER STATIONS

The PNW selects plot locations on maps, then transfers these plot locations to aerial photos using a radial line plotter or stereopotter. This procedure is considered too expensive by many inventory foresters.

The Southern Forest Experiment Station locates sample plots on the most recent conventional aerial photographs and establishes them on the ground. Then assigns geographic coordinates to the nearest mile for each plot using a coordinatograph with a 7½-minute quadrangle. The cost of this method is considered rather high also.

The Southern Region establishes forest survey field plots on maps by a systematic grid. Then transfers these locations to aerial photos and establishes a cluster of photo plots on each photo containing a field plot.

The Northeastern Region locates samples directly on individual conventional photos. Then arranges samples systematically using three photo plots per photo print and randomly chooses ground plots by photo class.

A new way was needed to use these photos that would estimate forest area accurately. Forest Survey at the North Central Station approached the problem with the objectives to: (1) select plot locations on aerial photos that would avoid bias due to uneven photo intensity, (2) determine how to select the proper grid scale to represent the land area sampled, and (3) keep costs down. The method we developed is described below.

NORTH CENTRAL PROCEDURE

A township mosaic is assembled from individual conventional photos for each township in our Region instead of using single individual conventional photos. Next, township boundaries are transferred from maps of plat books to the mosaic (thus providing the gound control of the area). This compensates for overlap, sidelap, crab (apparent sidewise motion of an airplane headed into a cross-wind), and tilt (departure from the vertical position of the camera). The time spent to assemble one township is ½ to 1 hour. Then a systematic grid of plots is placed over the township mosiac. Therefore, sample plots are uniformly spaced and an equal number of plots is represented in each township.

In our Region differences in relief are not great and contracting companies usually deliver photos in the prescribed range, but the scale of photos varies. To compensate for this, we have many sets of grids with variations of scale from 1:15,000 to 1:42,000. The appropriate grid is selected to match the scale of the photo mosaic.

The township mosaic assembly corresponds closely to township area on the ground. To avoid too many of the plots falling on roads (north-south and east-west), the grid is turned 5 degrees to the left. In the eastern part of the United States where land area is not divided by the township and range system, other controls of land area could be used such as geological survey contour maps (U.S.G.S. quads).

RESULTS AND DISCUSSION

The assembled mosaic system allows us to locate plots systematically on the aerial photos, which minimizes the bias due to photography in photo plot sampling. We still cannot entirely eliminate small differences of relief and some distortion on the edge of the photos, but we do eliminate costs of the map-ground transfer process and believe that our statistical results are realistic.

LITERATURE CITED

Pope, Robert B., Bijan Payandeh, and David P. Paine. 1972. Photo plot bias. U.S. Dep. Agric. For. Serv. Res. Pap. PNW-145, 8 p. Pac. Northwest For. & Range Exp. Stn., Portland, Oregon.

Cost, Boel D. 1976. Accuracy and cost of several methods for geographically locating Forest Survey sample plots. U.S. Dep. Agric. For. Serv. Res. Note SE-234, 4 p. Southeast. For. Exp. Stn., Asheville, North Carolina.

Bickford, C. Allen. 1952. The sampling design used in the Forest Survey of the Northeast. J. For. 50:290-293.

ESTIMATING D.B.H. FROM STUMP DIMENSIONS

Gerhard Raile, *Research Forester,*
North Central Forest Experiment Station,
St. Paul, Minnesota

A means of estimating diameter at breast height (d.b.h.) from stump measurements has several applications: (1) the volume removed in cases of timber tresspass can be calculated using local volume tables, (2) diameter distributions and basal areas for sample plots or stands can be calculated if trees have been cut and the data were not previously recorded or were lost, and (3) removals from a large forest area can be calculated. The equations presented here were developed as part of the 1977 Minnesota forest inventory. The d.b.h. estimated by these equations was used as an input to other volume equations to make an estimate of the timber removed from Minnesota's forests.

Previous studies of d.b.h. and stump diameter relations in other regions of the country have included few tree species of interest in the north-central States or have not been done in a form easily adaptable to forest inventory computer processing. Several of these studies were published only as tables or charts (Rapraeger 1941, Cunningham *et al.* 1947), while others were based on a linear relation from a fixed stump height (Bones 1960, 1961). Stump height was used as a variable by Curtis and Arney (1977) for estimating d.b.h. of second-growth Douglas-fir in the Pacific Northwest. McClure (1968) used stump height in a model similar to the model used in our study but his equations and tables cover species found in the southeast.

METHODS

We collected data from 2,575 trees. These data were collected as part of forest product utilization studies conducted in conjunction with forest inventories in Michigan, Wisconsin, and Minnesota. Measurements were taken from random samples of felled trees at logging operations in these States. Along with the d.b.h. for each tree, the diameter outside bark (d.o.b.) was measured to the nearest 0.1 inch at half-foot intervals from 0.5 to 2.5 feet above the ground (table 1). If an abnormality, such as a bulge or fork, occured at the measurement height, the measurement was not taken.

Table 1. — *D.b.h. regression coefficients for tree species of the Lake States*

Species group	Trees	Observations	D.b.h. range	Coefficient A + 1.0
	Number		*Inches*	
White pine	34	138	9.4-33.0	1.07035
Red pine	98	392	3.4-22.6	1.05462
Jack pine	474	1918	4.9-19.4	1.04608
White spruce	51	117	5.0-18.4	1.01082
Black spruce	124	426	5.0-13.3	1.02679
Balsam fir	189	532	4.2-15.6	1.01367
Tamarack	7	14	7.2-9.2	1.01752
Northern white-cedar	97	194	5.2-17.2	.95610
Other softwoods	--	--	--	[1]1.04608
White oak	34	137	10.6-22.9	1.04427
Red & northern pin oak	107	425	6.3-30.6	1.05658
Hickory	--	--	--	[2]1.05658
Yellow birch	22	47	13.2-23.8	1.10481
Hard maple	89	239	5.7-24.2	1.05199
Soft maple	27	114	8.0-24.2	1.05199
Ash	31	218	7.4-24.7	1.05559
Balsam poplar, Bigtooth aspen	187	582	5.0-17.8	1.07897
Paper birch	189	795	5.0-13.8	1.05155
Quaking aspen	738	2706	5.0-20.5	1.06439
Basswood	25	99	9.8-26.7	1.07428
Elm	48	174	7.0-30.5	1.06734
Select hardwoods	4	20	8.1-11.7	1.10929
Other hardwoods	--	--	--	[3]1.06439
Noncommercial species	--	--	--	[3]1.06439
TOTAL	2,575	9,287	3.4-33.0	--

[1] Used the value for jack pine.
[2] Used the value for red oak.
[3] Used the value for quaking aspen.

RESULTS

Because the best estimate of d.b.h. is obtained by measuring stump diameter at the highest point on a given stump and stump heights vary so greatly, stump height was chosen as an independent variable along with d.o.b. Plotting the ratios of d.b.h. to d.o.b. suggests a model of the form:

$$\frac{\text{d.b.h.}}{\text{d.o.b.}} = A + B \cdot \ln(H) + C \cdot \text{d.o.b.} \cdot H$$

where, A,B, & C = regression parameters, and H = stump height at which d.o.b. was measured.

Then, we modified the equation as follows to make it usable for stump heights ranging from 0 to 4.5 feet, because the natural logarithm of zero is undefined.

$$\frac{\text{d.b.h.}}{\text{d.o.b.}} = 1 + A + B \cdot (\ln(H + 1.0) - \ln \cdot 5.5) + C \cdot \text{d.o.b.} \cdot (H\text{-}4.5)$$

where, A = the regression coefficient for a given species group, B + C = regression coefficients, H = stump height in feet, d.o.b. = stump diameter outside bark in inches at H, and d.b.h. = diameter at breast height in inches.

This modified regression model was fit using multiple linear regression with species groups as a dummy variable. The species included in each species group are listed below.

Common name	Scientific name
SOFTWOODS	
Eastern white pine	*Pinus strobus*
Red pine	*Pinus resinosa*
Jack pine	*Pinus banksiana*
White spruce	*Picea glauca*
Black spruce	*Picea mariana*
Balsam fir	*Abies balsamea* var. *balsamea*
Tamarack	*Larix laricina*
Northern white-cedar	*Thuja occidentalis*
Other softwoods	*Juniperus virginiana*
	all other softwoods
HARDWOODS	
Oaks	*Quercus alba*
	Quercus bicolor
	Quercus macrocarpa
Red oak	*Quercus rubra*
Northern pin oak	*Quercus ellipsoidalis*
Hickories	*Carya cordiformis*
	Carya ovata
Yellow birch	*Betula alleghaniensis*
Hard maples	*Acer nigrum*
	Acer saccharum
Soft maples	*Acer rubrum* var. *rubrum*
	Acer saccharinum
Ashes	*Fraxinus americana*
	Fraxinus nigra
	Fraxinus pennsylvanica
Balsam poplar	*Populus balsamifera*
Paper birch	*Betula papyrifera* var. *papyrifera*
Bigtooth aspen	*Populus grandidentata*
Quaking aspen	*Populus tremuloides*
American basswood	*Tilia americana*
Elms	*Ulmus americana*
	Ulmus rubra
	Ulmus thomassii
Select hardwoods	*Juglans cinerea*
	Juglans nigra
	Prunus serotina
Other hardwoods	*Acer negundo*
	Betula nigra
	Celtis occidentalis
	Populus deltoides
Noncommercial species	

The R^2 for the regression is 0.64616 and the standard error of estimate is 0.5955. The A + 1 species coefficients are given in table 1. The coefficients B and C equal 0.1273 and 0.001641, respectively.

Figure 1 illustrates the advantages of this model, which increases the taper in the lower section of the stump for large trees. For examples, the data for northern white-cedar, balsam poplar and bigtooth aspen, and ash have been put in table form (tables 2, 3, and 4). These tables may be used to find the estimated d.b.h.'s for these trees when the stump height and stump d.o.b. are known. When the stump diameter is in other than 1-inch increments, interpolate to estimate d.b.h. A graph could be used in the field as a quick method of estimating d.b.h. (fig.2).

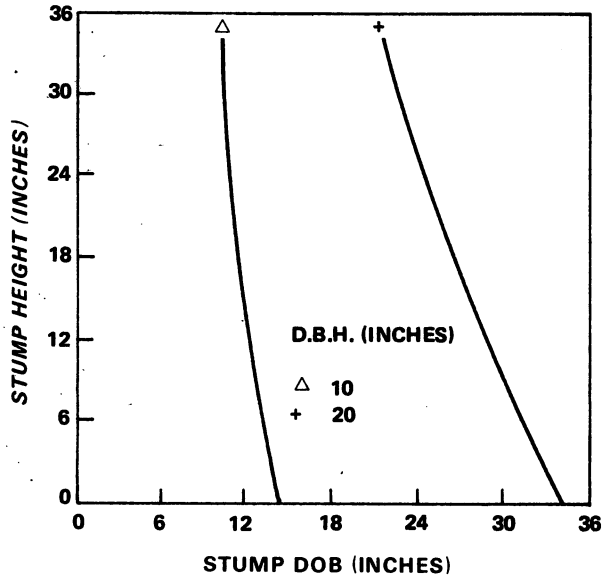

Figure 1. — *The relation of stump height and stump d.o.b. for 10- and 20-inch d.b.h. red pine.*

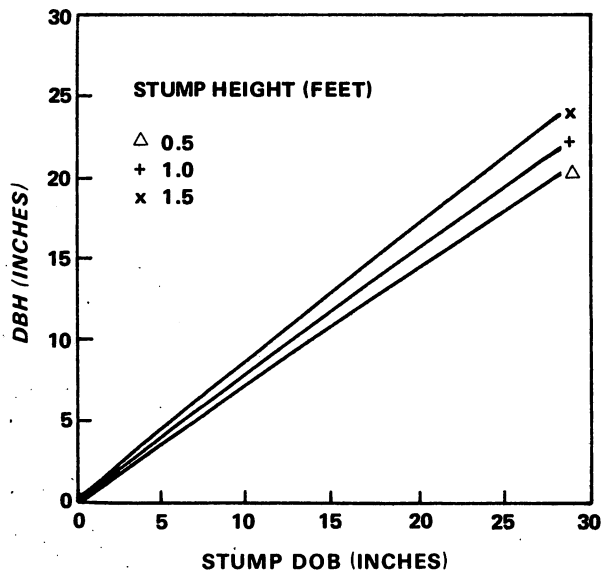

Figure 2. — *D.b.h. for red pine as a function of stump d.o.b.*

Table 2. — *Estimated d.b.h. for northern white-cedar from stump height and d.o.b.*
(In inches)

Stump d.o.b.	Stump height (feet) 0.5	1.0	1.5	2.0
5	3.8	4.0	4.2	4.3
6	4.5	4.8	5.0	5.1
7	5.2	5.5	5.7	6.0
8	5.9	6.3	6.5	6.8
9	6.6	7.0	7.3	7.6
10	7.3	7.7	8.1	8.4
11	7.9	8.4	8.8	9.2
12	8.5	9.1	9.6	10.0
13	9.2	9.8	10.3	10.7
14	9.8	10.5	11.0	11.5
15	10.4	11.1	11.7	12.3
16	11.0	11.8	12.4	13.0
17	11.5	12.4	13.1	13.8
18	12.1	13.0	13.8	14.5
19	12.7	13.6	14.5	15.2
20	13.2	14.2	15.1	15.9
21	13.7	14.8	15.8	16.6
22	14.2	15.4	16.4	17.4
23	14.7	16.0	17.1	18.0
24	15.2	16.5	17.7	18.7
25	15.7	17.1	18.3	19.4
26	16.1	17.6	18.9	20.1
27	16.6	18.2	19.5	20.7
28	17.0	18.7	20.1	21.4
29	17.4	19.2	20.7	22.0
30	17.8	19.7	21.2	22.7
31	18.2	20.1	21.8	23.3
32	18.6	20.6	22.3	23.9
33	18.9	21.0	22.9	24.5
34	19.3	21.5	23.4	25.1
35	19.6	21.9	23.9	25.7
36	20.0	22.3	24.4	26.3

Table 3. — *Estimated d.b.h. for bigtooth aspen and balsam poplar from stump height and d.o.b.*
(In inches)

Stump d.o.b.	Stump height (feet) 0.5	1.0	1.5	2.0
5	4.4	4.6	4.8	4.9
6	5.2	5.5	5.7	5.9
7	6.1	6.4	6.6	6.8
8	6.9	7.2	7.5	7.8
9	7.7	8.1	8.4	8.7
10	8.5	8.9	9.3	9.6
11	9.3	9.8	10.2	10.5
12	10.0	10.6	11.0	11.4
13	10.8	11.4	11.9	12.3
14	11.5	12.2	12.7	13.2
15	12.2	13.0	13.6	14.1
16	12.9	13.7	14.4	15.0
17	13.6	14.5	15.2	15.8
18	14.3	15.2	16.0	16.7
19	15.0	16.0	16.8	17.6
20	15.6	16.7	17.6	18.4
21	16.3	17.4	18.4	19.2
22	16.9	18.1	19.1	20.1
23	17.5	18.8	19.9	20.9
24	18.1	19.5	20.7	21.7
25	18.7	20.2	21.4	22.5
26	19.3	20.8	22.1	23.3
27	19.9	21.5	22.8	24.1
28	20.4	22.1	23.5	24.8
29	21.0	22.7	24.2	25.6
30	21.5	23.3	24.9	26.4
31	22.0	23.9	25.6	27.1
32	22.5	24.5	26.3	27.9
33	23.0	25.1	26.9	28.6
34	23.5	25.7	27.6	29.3
35	23.9	26.2	28.2	30.0
36	24.4	26.8	28.8	30.7

Table 4. — *Estimated d.b.h. for ash from stump height and d.o.b.*
(In inches)

Stump d.o.b.	Stump height (feet) 0.5	1.0	1.5	2.0
5	4.3	4.5	4.7	4.8
6	5.1	5.4	5.6	5.7
7	5.9	6.2	6.4	6.6
8	6.7	7.0	7.3	7.6
9	7.5	7.9	8.2	8.5
10	8.2	8.7	9.1	9.4
11	9.0	9.5	9.9	10.3
12	9.7	10.3	10.8	11.2
13	10.5	11.1	11.6	12.0
14	11.2	11.8	12.4	12.9
15	11.9	12.6	13.2	13.8
16	12.6	13.4	14.0	14.6
17	13.2	14.1	14.8	15.4
18	13.9	14.8	15.6	16.3
19	14.5	15.5	16.4	17.1
20	15.2	16.2	17.1	17.9
21	15.8	16.9	17.9	18.7
22	16.4	17.6	18.6	19.5
23	17.0	18.3	19.4	20.3
24	17.6	18.9	20.1	21.1
25	18.2	19.6	20.8	21.9
26	18.7	20.2	21.5	22.7
27	19.3	20.8	22.2	23.4
28	19.8	21.4	22.9	24.2
29	20.3	22.0	23.6	24.9
30	20.8	22.6	24.2	25.7
31	21.3	23.2	24.9	26.4
32	21.8	23.8	25.5	27.1
33	22.2	24.3	26.2	27.8
34	22.7	24.9	26.8	28.5
35	23.1	25.4	27.4	29.2
36	23.5	25.9	28.0	29.9

LITERATURE CITED

Bones, J. T. 1960. Estimating d.b.h. from stump diameter in the Pacific Northwest. U.S. Dep. Agric. For. Serv. Res. Note PNW-186, 2 p. Pac. Northwest For. & Range Exp. Stn., Portland, Oregon.

Bones, J. T. 1961. Estimating spruce and hemlock d.b.h. from stump diameter. U.S. Dep. Agric. For. Serv. Tech. Note 51,2 p. North. For. Exp. Stn., Juneau, Alaska.

Cunningham, F. E., S. M. Filip, and M. J. Ferree. 1947. Relation of tree stump diameter to diameter breast high. U.S. Dep. Agric. For. Serv. Stn. Note 1, 3 p. Northeast. For. Exp. Stn., Philadelphia, Pennsylvania.

Curtis, Robert O., and James D. Arney. 1977. Estimating d.b.h. from stump diameters in second-growth Douglas-fir. U.S. Dep. Agric. For. Serv. Res. Note PNW-297, 7 p. Pac. Northwest For. & Range Exp. Stn., Portland, Oregon.

McClure, Joe P. 1968. Predicting tree d.b.h. from stump measurements in the southeast. U.S. Dep. Agric. For. Serv. Res. Note SE-99, 4 p. Southeast. For. Exp. Stn., Asheville, North Carolina.

Rapraeger, E. F. 1941. Determining tree d.b.h. from stump measurements. U.S. Dep. Agric. For. Serv. Res. Note 16, 6 p. North. Rocky Mtn. For. & Range Exp. Stn., Missoula, Montana.

☆U.S. GOVERNMENT PRINTING OFFICE: 1978-666-042/124 REG.#6

U.S. Department of Agriculture, Forest Service.
1978. Proceedings 1977 Midwest Forest Mensurationists Meeting. U.S. Dep. Agric. For. Serv. Gen. Tech. Rep. NC-46, 34 p. North Cent. For. Exp. Stn., St. Paul, Minnesota.

Contains 6 papers presented at the 1977 meeting of the Midwest Mensurationists.

OXFORD: 5:(081). KEY WORDS: sequential sampling plans, Monte Carlo simulation, stand stocking, individual tree growth, diameter distribution, aerial photo intensity, volume.

U.S. Department of Agriculture, Forest Service.
1978. Proceedings 1977 Midwest Forest Mensurationists Meeting. U.S. Dep. Agric. For. Serv. Gen. Tech. Rep. NC-46, 34 p. North Cent. For. Exp. Stn., St. Paul, Minnesota.

Contains 6 papers presented at the 1977 meeting of the Midwest Mensurationists.

OXFORD: 5:(081). KEY WORDS: sequential sampling plans, Monte Carlo simulation, stand stocking, individual tree growth, diameter distribution, aerial photo intensity, volume.

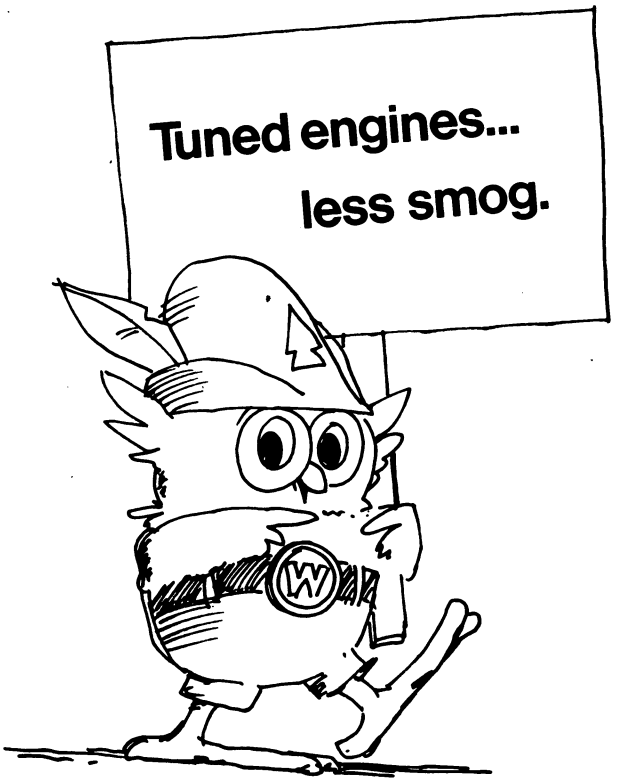
Tuned engines...
less smog.